Università
Ca'Foscari
Venezia

Master's Degree in
Environmental Sciences

*Final Thesis*

# Exploring fire activity during the Holocene using Antarctic ice cores

**Supervisor**
Ch. Prof. Carlo Barbante

**Co-supervisor**
Prof. Dario Battistel

**Graduand**
Sierra Grange
877327

**Academic Year**
2019/2020

## Table of Contents

**List of Figures** ..... **3**

**List of Tables** ..... **5**

**Abstract** ..... **6**

**1. Introduction** ..... **7**

1.1 Reconstructing Fire History ..... 7
1.2 Primary Data Sources ..... 7
1.3 Charcoal in Lakes ..... 8
1.4 Black Carbon in Polar Regions ..... 10
1.5 Levoglucosan ..... 12

**2. Aim** ..... **15**

**3. Methods** ..... **16**

3.1 Holocene ..... 16
3.2 Study Site ..... 16
3.3 Regional settings ..... 17
3.4 Levoglucosan sample collection ..... 17
3.5 Levoglucosan analysis ..... 18
3.6 Detection limits ..... 19
3.7 Charcoal record ..... 19
3.8 Packages and tools for evaluation ..... 20
3.9 Age/depth model ..... 20

**4. Results** ..... **21**

4.1 Statistical analysis of the levoglucosan record ..... 21
4.2 Charcoal Synthesis ..... 26
4.3 Identification of phases ..... 29

**5. Discussion** ..... **33**

5.1 Atmospheric Transport ..... 33
5.2 Vegetation during the Holocene ..... 34
5.3 Climatic Variables ..... 36
5.4 Orbital Parameters ..... 39
5.5 Charcoal correlation ..... 42
5.6 Levoglucosan phases ..... 42

**6. Conclusion** ..... **45**

**Bibliography** ..... **46**

## List of Figures

**Figure 1.** The three drivers needed for a single fire event versus the three drivers required for a fire regime. Marlon (2020). ..... 7
**Figure 2.** Model of black carbon flux in comparison to seven ice cores. Arienzo et al. (2017). ..... 11
**Figure 3.** Map of Antarctic ice core locations. The location of interest is marked as EDC. Schoenemann et al. (2014). ..... 16
**Figure 4.** Levoglucosan concentration data set with no transformations. ..... 21
**Figure 5.** Levoglucosan concentration data set with no transformations reported in yr BP. ..... 22
**Figure 6.** (a) Levoglucosan record with no anomalies and having undergone a log transformation. (b) Histogram of log-transformed levoglucosan record. ..... 23
**Figure 7.** (a) LOESS regression using .2 as the span parameter and concentration as the target variable. (b) LOESS regression using .75 as the span parameter and concentration as the target variable. ..... 24
**Figure 8.** (a) Levoglucosan concentration with potential outliers and megafires calculated using criterion (I). (b) Levoglucosan concentration with potential outliers and megafires calculated using criterion (II). ..... 25
**Figure 9.** Charcoal synthesis of (a) Southern Hemisphere, (b) South America, (c) Africa, (d) Australia and New Zealand. Blue circles represent unselected GCD sites, and red dots represent the selected sites. ..... 27
**Figure 10.** The correlation between levoglucosan recorded at EDC and the charcoal synthesis from the Southern Hemisphere (SH), South America (SA), Africa, and Australia/New Zealand (Aus). ..... 28
**Figure 11.** The seven phases of the levoglucosan flux. Please note the changes in the axes. (a) Phase 1 of the levoglucosan record spanning from 38 yr BP to 3672 yr BP. (b) Phase 2 of the levoglucosan record spanning from 3709 yr BP to 4019 yr BP. (c) Phase 3 of the levoglucosan record spanning from 4057 yr BP to 7498 yr BP. (d) Phase 4 of the levoglucosan record spanning from 7539 yr BP to 8319 yr BP. (e) Phase 5 of the levoglucosan record spanning from 8361 yr BP to 9207 yr BP. (f) Phase 6 of the levoglucosan record spanning from 9242 yr BP to 9652 yr BP. (g) Phase 7 of the levoglucosan record spanning from 9686 yr BP to 10479 yr BP. ..... 30
**Figure 12.** Phase 1 of the levoglucosan record spanning from 38 yr BP to 3672 yr BP. Phase 2 of the levoglucosan record spanning from 3709 yr BP to 4019 yr BP. Phase 3 of the levoglucosan record spanning from 4057 yr BP to 7498 yr BP. Phase 4 of the levoglucosan record spanning from 7539 yr BP to 8319 yr BP. Phase 5 of the levoglucosan record spanning from 8361 yr BP to 9207 yr BP. Phase 6 of the levoglucosan record spanning from 9242 yr BP to 9652 yr BP. Phase 7 of the levoglucosan record spanning from 9686 yr BP to 10479 yr BP. ..... 32
**Figure 13.** Probability that within the last 10 days air has arrived from the stratosphere and entered the lowest 500 m in both spring and fall. Spring is defined as September, October, and November and fall is defined as March, April, and May. Stohl and Sodemann (2010). ..... 33
**Figure 14.** Potential source contributions of black carbon from biomass burning in both winter and summer. The particles had to spend a minimum of five days in the Antarctic and reach an altitude of at least 1000 m above sea level. Stohl and Sodemann (2010). ..... 34

**Figure 15.** Vegetation maps produced by BIOME 6000 comparing the vegetation patterns from 0 ka and 6 ka. Harrison and Prentice (2003). 35
**Figure 16.** Methane ($\delta^{13}CH_4$) levels from GISP2 in Greenland, TALDICE, EDML, and EDC in Antarctica. These records have been measured with no krypton interference. Bock et al. (2017). 37
**Figure 17.** a) Geopotential height anomalies that occur during a) La Niña and b) El Niño. Markle et al. (2012). 38
**Figure 18.** a) Geopotential height anomalies that occur during a) Positive SAM and b) Negative SAM. Markle et al. (2012). 39
**Figure 19.** Orbital parameters a) obliquity, b) eccentricity, and c) precession throughout the Holocene. 41
**Figure 20.** Temperature anomalies between 60°S-30°S. May (2017). 43
**Figure 21.** Earliest agriculture onset at the common prevalence level which is 1-20% of the land area. Stephens et al. (2019). 44

## List of Tables

**Table 1.** Model of black carbon flux in comparison to seven ice cores. Kuo et al. (2008). ..... 13

**Table 2.** Correlation coefficient through the five selected time intervals of the Southern Hemisphere, South America, Africa, and Australia/New Zealand. The p-value is based on the usual significance level, alpha = 0.05. If the p-value is <0.05 (red), the correlation is considered significant. If the p-value is >0.05 (black), the correlation is not considered significant. ..... 29

**Table 3.** Welch Two Sample t-test results based on the usual significance level, alpha = 0.05. If the test is considered statistically different (red), there is a difference between the true averages. If the test is not statistically different (black), there is no difference between the true averages. ..... 31

**Table 4.** Natural budgets of methane throughout the Last Glacial Maximum, Pre-industrial Holocene, and up to 1993. Chappellaz et al. (1993). ..... 36

## Abstract

The understanding of the fire regime, the pattern and frequency of fires, and how it changes throughout Earth's history can help us to form a connection between climate variability, vegetation fluctuation within biomes, and anthropogenic activity. These three variables impact fire patterns which in turn impact the atmosphere. By reconstructing the paleofire record we can better assess the paleoclimate and address the drivers of climate change in our past, and therefore better predict the drivers of the future.

This work evaluates the relationship between climate variability and fire occurrence in the Southern Hemisphere during the Holocene using levoglucosan, an anhydrous sugar formed from the pyrolysis of cellulose, collected from EPICA Dome C in Antarctica. Once the ice core had been collected and the levoglucosan samples were measured, the record underwent analysis. First the levoglucosan record was considered and observed on its own, undergoing several calculations and transformations to identify potential megafires or outliers. Next charcoal records obtained from the Global Charcoal Database (GCD) were synthesized and added to the analysis in an attempt to observe long-term trends in fire activity.

In conclusion, the fire activity due to natural fire contributors such as the temperature, orbital parameters, El Niño-Southern Oscillation (ENSO), Southern Annular Mode (SAM), and $CO_2$ is notable throughout the Early Holocene. However, the fire signal appears to move away from a natural stability possibly towards a more anthropogenic signal as we enter the late Holocene (3000 yr BP – present).

# 1. Introduction

## 1.1 Reconstructing Fire History

A fire requires oxygen, heat, and fuel. Without these three seemingly simple ingredients, it cannot start. In addition, a fire regime, or a pattern of fires, needs to take climate, vegetation, and human activities into account (Figure 1) (Marlon, 2020). A host of metrics, such as seasonality, frequency, size, location, or how much it consumed can make up the regime, further complicating the ecology and understanding of fires.


***Figure 1.*** *The three drivers needed for a single fire event versus the three drivers required for a fire regime. Marlon (2020).*

The analysis of these regime changes allows the reconstruction of the history of the links between climate, human activities, and vegetation. By studying the variations and connections within the fire regime drivers throughout Earth's history we may lessen our chances of understanding specific fire events, but we can gain insight into larger changing patterns (Marlon, 2020). We will need to track these changes by employing one or more data source. Satellites, written records, fire-scarring on trees, and geochemical tracers formed from combustion residue found in sediment and ice are the four primary sources that can be used to analyze past wildfires (Marlon, 2020).

## 1.2 Primary Data Sources

When considering "recent global fire activity," fire activity occurring presently or within the past few decades, satellite remote-sensing systems can be utilized (Marlon, 2020). These

systems collect a variety of data from both regional and global scopes in order to estimate the amount of particulates and trace gases that have been emitted (Marlon, 2020).
In addition to satellites, historical fire data such as aerial photos, field studies, government records, and statistics reported through government agencies can be employed to compile general trends at a variety of levels dependent on the area considered (Marlon, 2020).
If a fire-scarred shrub or tree can be accurately dated, the dendrochronological data can be used to understand past wildfires intensity and frequency (Marlon, 2020). The records gathered from accurately dated tree rings in different wooded environments can provide information on the average fire return intervals over a broad time period, or the relationship between specific fire events and drought conditions.
However, of the four primary sources available, paleofire data sources consist of several different types of geochemical tracers such as charcoal, black carbon, and levoglucosan.

### 1.3 Charcoal in Lakes

To track the fire regime changes and the link with the climate variability over centennial to millennial time scales, sedimentary charcoal records have been widely employed during the last decades. They have the advantage of spanning back further in time and covering more area than dendrochronological fire records allow (Marlon et al., 2013).
The burning of biomass does not only result in the release of gases such as nitrous oxide, methane, carbon dioxide, and carbon monoxide (Marlon et al., 2013). Incomplete combustion will also cause soot and charcoal particulates to form when there is not enough oxygen to completely react with the burning biomass. These charcoal particles are then subject to the elements. Both surface runoff, the flow of water unable to penetrate the surface, and wind are responsible for transporting the charcoal particles into the depositional environment, such as lakes, bogs, or soil profiles (Power et al., 2010). The distance the charcoal can be transported depends on three different main factors: mode of transportation, the type of depositional environment or sedimentary basin, and the size of the particle (Power et al., 2010). Shifts in wind as well as varying amounts of surface runoff directly impact how much charcoal is transported into the sedimentary basin. Smaller charcoal particles (<50 µm) can travel long distances. Therefore, with respect to the diffusion of emissions, there is likely to be overrepresentation of regional fire events (Power

et al., 2010). This is particularly true if the sedimentary basin is greater than 50 $km^2$, as a large basin provides more opportunities to capture regional charcoal particulates (Power et al., 2010).

Due to the implementation of the Global Charcoal Database (GCD), we have access to hundreds of charcoal records that cover the past 11,700 years, a period known as the Holocene (Power et al., 2010). The records found in this database can be used to gain insight into fire history and how the fire regime has evolved, as well as the relationship between the climate, humans, and fire (Power et al., 2010). Further studies are required to ensure that all the information needed to fully understand the links between the creation, transportation, and deposition into different depositional environments is available (Power et al., 2010).

Lakes and similar sedimentary basins are attractive options as archives due to their ability to continuously accrue matter (Power et al., 2010). However, lake sites present several potential problems. While our knowledge of charcoal taphonomy has increased in the last 30 years, it is necessary to conduct more studies on the available calibration techniques (Power et al., 2010). Charcoal taphonomy may be affected by varying fuel loads and distribution, making some results inconclusive (Power et al., 2010). In addition to the questions of distribution as far as taphonomy is concerned, there is an issue of distribution when it comes to the sedimentary basins in question. Lakes are not evenly distributed as 50% of the world's lakes are located in Canada (Cael and Seekell, 2016). Mountainous regions and areas of high latitude are likely to be overrepresented within the fire history as many of the world's lakes can be found there (Cael and Seekell, 2016). Not only are they unevenly distributed in location, but they are also skewed in size-distribution as well (Cael and Seekell, 2016). As Power et al. (2010) concluded, a large basin (>50$km^2$) provides more opportunities to capture regional charcoal particulates. This leaves a significant chance for overrepresentation. As most of the world's lakes are found in the northern hemisphere, an adequate global view cannot be gained by looking to records of charcoal found in lakes (Cael and Seekell, 2016).

### 1.4 Black Carbon in Polar Regions

While carbon dioxide is the most important anthropogenic radiative-forcing agent, black carbon is the second (Arienzo et al., 2017). This radiative forcing, or the alterations to the Earth's radiative equilibrium, cause a shift in the absorption of sunlight within the atmosphere (Bond et al., 2013). As black carbon plays such a significant role within the atmosphere, using it to understand paleofire records and observe the links between black carbon emissions, biomass burning, and our climate is a logical practice (Arienzo et al., 2017).

Black carbon refers to a collection of carbonaceous material that is formed when there is an incomplete combustion of biomass, such as plant tissue, or when graphitized soot is made within the fire (Shrestha et al., 2010). Definitions of black carbon based upon both physical and chemical properties have been suggested, however, it must be noted that black carbon lacks a universal chemical definition (Long et al., 2013). The ratio of carbon, hydrogen, and nitrogen varies, but on average black carbon is 60% carbon with the remainder being an amalgamation of oxygen, sulfur, nitrogen, and hydrogen (Shrestha et al., 2010). The physical properties have been more clearly defined, but still lack a solid consensus. Black carbon keeps its form even at high temperatures, only vaporizing near 4000K; strongly absorbs visible light; and is poorly soluble (Long et al., 2013; Bond et al., 2013).

Black carbon's global origins are easier to understand than its chemical makeup. Fires located in forests and savannahs represent the largest global source of black carbon, but when it comes to other means of emission, the top source is region specific (Bond et al., 2013). The largest contributor for Europe, North America, and Latin America are diesel engines with 70% of emissions (Bond et al., 2013). In Asia and Africa burning solid fuels for heat or cooking makes up 60 to 80% of black carbon emissions (Bond et al., 2013). The greatest contribution in Post-Soviet States, some Eastern European countries, and China is residential coal (Bond et al., 2013). Shipping and aviation emit a significantly lower amount of black carbon and represent only a small portion, 9%, of the global scale (Bond et al., 2013).

Coastal Antarctica is subject to a strong circumpolar current known as the Antarctic Circumpolar Current, or the ACC (Chaubey et al., 2010). Driven by strong westerly winds, this current, estimated to be between 100-150 million $m^3/s$, must counteract the force of the

wind (Rintoul et al., 2001). The winds that drive this current can account for some of the deposition that occurs in Antarctica as both wet and dry deposition can occur via wind. Arienzo et al. (2017) states that wet deposition, as a result of precipitation scavenging, is largely responsible for black carbon deposition. However, the accumulation rates decrease and as shown in Figure 2, we observe a lower black carbon flux as we move inland from the coastal region (Arienzo et al., 2017). Therefore, the sites cannot be considered homogeneously distributed and the sites located on the coast are overrepresented (Arienzo et al., 2017).

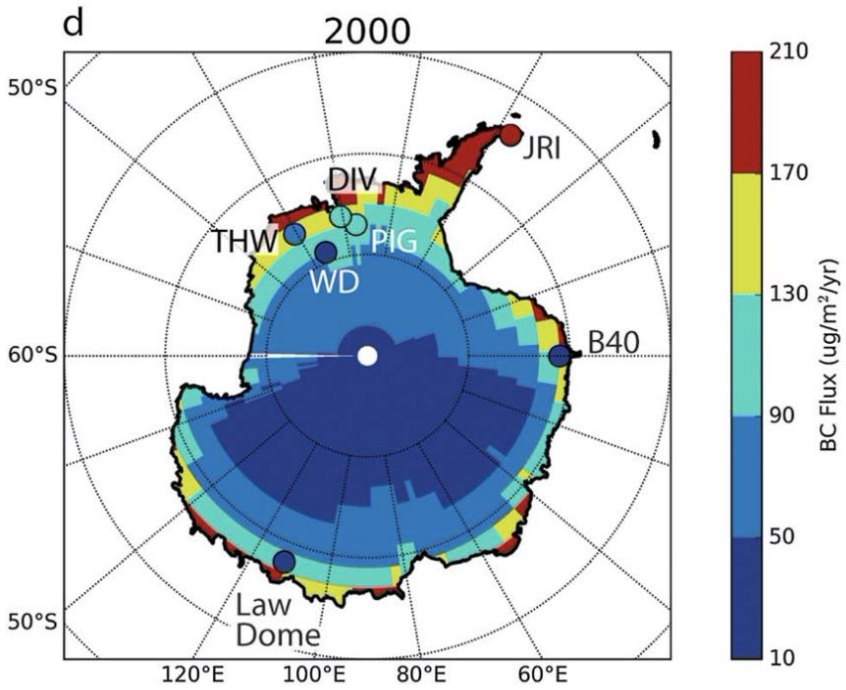


***Figure 2.*** *Model of black carbon flux in comparison to seven ice cores. Arienzo et al. (2017).*

The areas from which the black carbon can be sourced are also not homogenously distributed. South America is the dominant source of black carbon to Antarctica as indicated by modern observations and model simulations (Arienzo et al., 2017). Although, when considering different sites, we can see different dominant sources. Black carbon in eastern Antarctica is primarily sourced from Central Brazil as indicated by measurements from the Troll Research Station (Arienzo et al., 2017). Measurements taken at Syowa Station lead us to note that South America and southern Africa are the predominate sources (Arienzo et al., 2017). With the potential for sub-annual to annual resolution, polar ice core records can be

precisely dated, unlike charcoal records obtained from lakes (Arienzo et al., 2017). In further contrast to lake archives, the deposition of black carbon is not subjected to alteration or postdeposition mixing (Arienzo et al., 2017). Additionally, the ice core is located at a considerable distance from the burning biomass, indicating a regional record rather than a local record of emissions (Arienzo et al., 2017). However, this does not indicate that black carbon alone is an adequate proxy for reconstructing fire history. Arienzo et al. notes that when taking different regions in South America, the heterogeneous fire response cannot be recorded as there are marked differences when considering larger regions (Arienzo et al., 2017). Furthermore, the methodology in measurements vary widely leading to a large margin of error and fluid interpretation of results. As black carbon may vary chemically, different methods of detection may be augmented towards a particular chemical makeup (Hammes et al., 2007).

### 1.5 Levoglucosan

Although previous studies have indicated that the Antarctic region was affected by biomass burning due to the presence of black carbon, the presence of levoglucosan can confirm that it is not only due to local pollution (Hu et al., 2013). When biomass is burned it does not only release gases and particulates such as black carbon, it also produces levoglucosan (1.6-anhydro-b-D-glucopyranose), an anhydrous sugar (Itabaiana et al., 2020). This molecular tracer is a noteworthy choice as it can only be produced during a combustive process and unlike the burning of petroleum products or coal; which may result in a number of pollutants such as carbon monoxide, carbon dioxide, sulfur, nitrogen dioxide, nitric oxide, volatile organic compounds, and hydrocarbons; levoglucosan can only be found in biomass combustion residues, as shown in Table 1 (Kuo et al., 2008; Sajwan et al., 2006).

***Table 1.*** *Model of black carbon flux in comparison to seven ice cores. Kuo et al. (2008).*

Levoglucosan concentration in different environmental materials

| Material | Description | Levoglucosan (μg/g) | *n* |
|---|---|---|---|
| SRM 2975 | Diesel particulate matter | BDL[b] | 2 |
| ANL[a] coals | Pittsburgh bituminous coal, Pocahontas bituminous coal, Blind canyon bituminous coal, and Beulah-Zap lignite | BDL | 2[c] |
| SRM 1632c | Bituminous coal | BDL | 3 |
| Melanoidin | Urea-glucose melanoidin | BDL | 1 |
| Carbon black | Acetylene black | BDL | 2 |
| Lampblack | Crude oil combustion residue | BDL | 2 |
| SRM 1944 | NY/NJ water way sediment | BDL | 2 |
| Activated carbon | Commercial product from plant combustion | BDL | 2 |
| Char-BC 1 | Chestnut wood char | BDL | 2 |
| Char-BC 2 | Rice straw char | 14.7 ± 0.8 | 2 |
| Natural charcoal | Pine wood char | 69.4 ± 12.5 | 2 |
| Pre-fire soil | Surface soils from controlled burning site in New Mexico (US) | 0.85 ± 0.01 | 2 |
| Post-fire soil | | 38.0 ± 11.7 | 2 |
| SRM 1649a | Urban dust | 163.9 ± 11.8 | 11 |
| RM 8785 | Air particulate matter (PM2.5) on filter media | 158.4 ± 8.8 | 2 |
| Chimney soot | Chimney residues from Texas (US) private residence | 26888.1 | 1 |

[a] Argonne National Laboratory (ANL).
[b] Below detection limit (BDL).
[c] $n = 2$ for each coal standard.

This specificity allows us to rule out the regional specific emissions such as diesel engines and enables us to focus solely on the burning of biomass that would have occurred during paleofire events. With a high emission factor and relative stability within the atmosphere, levoglucosan can be considered an ideal tracer (Hu et al., 2013).

The chemical information from the past two millennia contained inside ice cores in Greenland identify boreal forests in Eurasia and North America to be the important sources of biomass burning (Zennaro et al., 2008). This data, in combination with the information provided by the global charcoal database has helped to reconstruct the fire activity during the Holocene. In Greenland, Zennaro et al. (2008) concluded that the fluctuation in levoglucosan cannot be explained by drastic temperature or environmental changes. These results are indicative of an increase in human-related fire activity (Zennaro et al., 2008). To ensure these results are truly global we need to look to the Southern Hemisphere.

A study conducted by Hu et al. found that the level of levoglucosan in both the Northern and Southern Hemispheres was not significantly different (Hu et al., 2013). Much like charcoal and black carbon, Hu et al. states that atmospheric circulation, deposition, degradation, and emissions all have a role in the concentration of levoglucosan in the atmosphere (Hu et al., 2013). While transport also plays a role in the levoglucosan concentration, especially taking the atmospheric circulation of the Antarctic into consideration, this will be discussed in greater detail in the following sections.

Understanding the fluctuation of levoglucosan throughout the past is vital to assessing the current atmospheric levels of levoglucosan (Gambaro et al., 2008). This can be accomplished

by carefully selecting the appropriate archive. Greater precision with dating, no post-depositional mixing, and the benefit of an established accumulation rate allowing for an easily calculable flux are all advantages that can be attributed to ice cores (Gambaro et al., 2008). In order to reconstruct paleofire history, we can utilize the chemical information stored in Antarctic ice cores along with levoglucosan data, and in doing so, continue piecing together the paleoclimate.

## 2. Aim

In this thesis I aim to use an ice core section collected from EPICA Dome C (EDC) in Antarctica to evaluate the dynamics of the fire regime during the Holocene. Levoglucosan, an anhydrous sugar, is a specific burning biomarker that can only be produced through the combustion of cellulose. The ice core collected from EDC was previously analyzed at Ca' Foscari, providing a high-resolution fire record at a Hemispherical scale. The levoglucosan record that was obtained is available as raw data, and in need of further elaborations that are not yet available. In this thesis I aim to improve the analysis of this record by evaluating the presence of possible outliers that may be representative of megafire events, an error of measurement, or an increased period of highly efficient transport. To correlate the findings and further our understanding of past fire regimes, charcoal records will then be synthesized and analyzed. Moreover, the temporal trend of levoglucosan will be compared with various climatic variables in order to evaluate the natural and the anthropogenic contributions to the fire occurrence in the Southern Hemisphere during the Holocene.

# 3. Methods

## 3.1 Holocene

Around 10,000 radiocarbon ($^{14}C$) years, or 11,700 calendar years ago, the Earth entered its most recent interglacial interval known as the Holocene (Roberts, 1999; Agenbroad et al.,2018). The Holocene is the youngest of the two epochs that make up the Quaternary period (Agenbroad et al., 2018). Geologically the Holocene is considered unique as this epoch contains a variety of correlating deposits, and these can be used to establish a timeline with the help of an age-depth model (Agenbroad et al., 2018).

## 3.2 Study Site

Located at 75°05'59"S 123°19'56"E and 3233 m above sea level, EPICA Dome C (EDC) is a dome, or flat snow summit, on the Antarctic Plateau (Stenni et al., 2010; Dargaud, 2004).

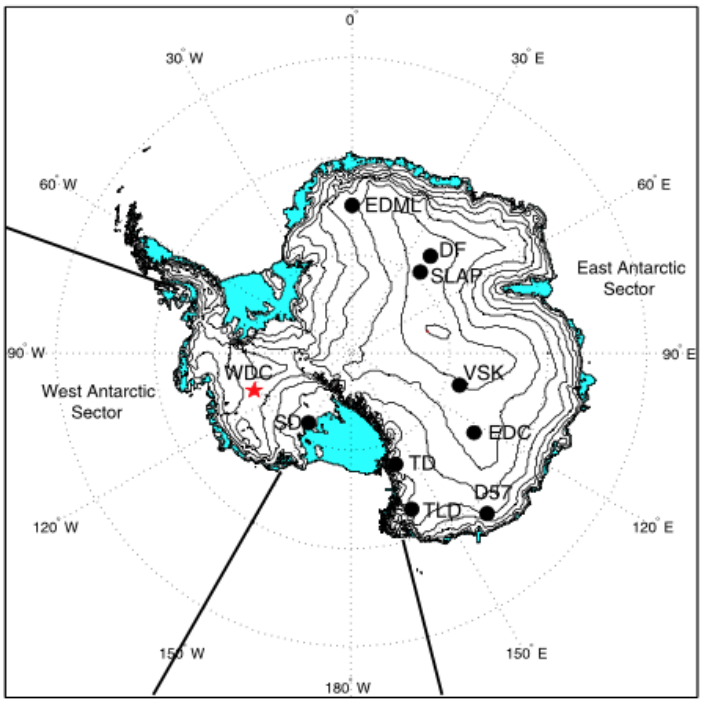


***Figure 3.*** *Map of Antarctic ice core locations. The location of interest is marked as EDC. Schoenemann et al. (2014).*

EDC ice cores were drilled from 1993-2004 according to a report completed in 2011 by Masson-Delmotte et al. EDC experiences a mean average temperature of -54.5°C and a relatively low amount of accumulation at about 25 kg $m^{-2}$ $yr^{-1}$ (Masson-Delmotte et al., 2011). As the annual layer thickness is small, layer counting is not feasible (Parrenin et al.,

2007). A firn densification model completed by Loulergue et al. (2007) calculated the gas age at both EDC and EDML, while Raisbeck et al. (2007), used the beryllium-10 peak found at 41 kyr in the EDC ice core to tie it into the NorthGRIP core's chronology, allowing EDC to be accurately dated (2007).

### 3.3 Regional settings

Levoglucosan concentration in the atmosphere is determined by the deposition and degradation that occurs during transport as well as the atmospheric circulation (Hu et al., 2013). The unique circulation in and around Antarctica plays a direct role in determining the transport potential from biomass burning sources. As EDC is located in the east, focus can be drawn to circulation patterns that impact East Antarctica (Hu et al., 2013).

The Antarctic Circumpolar Trough (ACT), a low-pressure belt located at approximately 64°S, divides the atmospheric circulation into two sections (Hu et al., 2013). This trough is characterized by intense cyclonic activity (Markle et al., 2012). Areas north of this divide experience westerly winds, while areas south of the divide experience easterly winds (Hu et al., 2013). The westerly winds drive what is known as the Antarctic Circumpolar Current eastward around the globe (Parish & Bromwich, 2007).

Acting as a competing influence on the cyclonic ACT are the anticyclonic and fairly high-pressured katabatic winds, or drainage winds, which are common to Antarctica (Markle et al., 2012; Parish & Cassano, 2003). These winds descend down a slope that has been affected by radiative cooling (Parish & Cassano, 2003). As there is an inverse relationship between temperature and air density, it follows that the air being displaced by the katabatic winds is warmer than the wind itself (Parish & Cassano, 2003). A further result of this inverse relationship is that the origin of the katabatic winds is not contingent on the orientation of the horizontal pressure gradient force in the free atmosphere (Parish & Cassano, 2003). Overall, the topographic slope and the orientation of the ice sheets are the primary influencers of the winds in Antarctica (Parish & Bromwich, 2007).

### 3.4 Levoglucosan sample collection

Using an electromechanical drill, cylindrical samples 10 cm in diameter and 55 cm long were collected from EDC. Due to the nature of the drilling, the retaining wall contaminates the

outside of the ice core with heavy metals and organic compounds. Decontamination was conducted at the Laboratory of Glaciology and Geophysics of the Environment (LGGE) by removing the external layers of the ice core with a Class 100 laminar flow clean bench. What remained was an uncontaminated inner core which was split into two pieces, melted, and stored in ultraclean low-density polyethylene (LDPE) bottles where they were refrozen until they were analyzed. To lower the risk of contamination, a minimalized sample preparation in a Class 100 clean chemistry laboratory was developed and followed. Ultrapure water was used to wash every LDPE vial or bottle, next an ultrasonic bath was used to clean the aforementioned bottles and vials three times, after which they were stored in plastic bags until use, before which they were rinsed again. Further details are reported in Gambaro et al., 2008.

### 3.5 Levoglucosan analysis

Analysis of the sample began immediately after 25 $\mu$L of a 1.41 ng mL$^{-1}$ levoglucosan $^{13}$C was mixed with 675 $\mu$L of melted ice in ultrapure water following the analytical method proposed by Gambaro et al., 2008. Two methods of analysis were jointly employed, liquid chromatography and negative ion electrospray ionization by way of mass spectrometry (HPLC/(-)ESI-MS/MS). To complete the liquid chromatographic analysis, 100 $\mu$L of the sample was injected onto a C18 Synergy Hydro column. 180 $\mu$L min$^{-1}$ using a 15% v/v methanol solution in water was then used as the composition remained constant throughout the HPLC separation indicating an isocratic elution. An ammonium hydroxide solution was then added at a flow of 5 $\mu$L min$^{-1}$ which resulted in a 1.5 minute retention time for the levoglucosan. To determine the levoglucosan levels in the ice, a mass spectrometer was used. Multiple reaction monitoring allowed the data to be collected in negative ion mode. For this method to be successful two parameters, collision energy and collision cell exit potential, were considered and optimized by directly infusing the ion source of the mass spectrometer with 500 ng mL$^{-1}$ solution of levoglucosan in ultrapure water. In the analysis of the peaks provided by the chromatography, the results showed that the peak from the ice samples was mostly due to levoglucosan (Gambaro et al., 2008). This is evident because of the low intensity of the *m*/*z* 161/87 and 161/129 transitions which

occur when galactosan and mannosan, two important compounds that result from burning biomass, are present.

### 3.6 Detection limits

The concentration of levoglucosan in the ice cores is very low (picogram per milliliter), requiring special care to optimize analysis and determine the limit of detection (LOD), as demonstrated by Gambaro et al., 2008 who analyzed six samples of levoglucosan in ultrapure water to evaluate the procedural blanks. LOD was determined as the standard deviation of the six procedural blanks multiplied by 3, resulting in a mean value of 3 pg $mL^{-1}$. Gambaro et al.'s (2008) study showed that the LOD and sensitivity results are excellent when using (HPLC/(-)ESI-MS/MS). This is further confirmed when the levoglucosan concentrations are considered. The minimum levoglucosan concentrations from the glacial ice samples are, in general, greater than the LOD and the interglacial samples are comparable to the LOD (Gambaro et al., 2008).

### 3.7 Charcoal record

To further our understanding of past fire regimes and correlate the data provided by levoglucosan analysis, we can use charcoal records obtained from a continental archive, such as lacustrine sediments (Battistel et al., 2018). The charcoal records used in this paper were obtained using the datasets provided by the Global Charcoal Database (GCD) and the paleofire package found in R (Blarquez et al., 2014). The paleofire package is particularly useful as it analyzes and synthesizes the charcoal time series found in the GCD (Blarquez et al., 2014). The Global Paleofire Working Group team started this initiative to transform the charcoal data if needed and provide site selection, thereby allowing customized charcoal syntheses (Blarquez et al., 2014; Battistel et al., 2018).

While it is logical that biome distribution continues to change, the proportion of Global Charcoal Database (GCD) grassland sites compared to the modern continent or global distribution is unequal. When compared with South America, Africa, and Eurasia; North America and Oceania have more paleofire records (Berangere et al., 2018). Records within these continents also vary widely due to protected environments, political instability,

limited depositional environments, or because of difficulty reaching a potential site as a consequence of its remote nature (Berangere et al., 2018).

When studying the temporal changes between forest and nonforest environments, pollen records are essential. However, pollen records are limited in grass-dominated landscapes for a myriad of reasons including differing grass pollen types as well as the lack of evenly distributed records through time and space. It is for these reasons that no reconstruction has been made in relation to the way a forest or grassland fire would register within the charcoal record. In areas with a fairly developed record, most sites appear to be located on the border of grasslands or among a forested area, so more paleofire records must be developed within grassland environments (Berangere et al., 2018).

### 3.8 Packages and tools for evaluation

The data obtained from the levoglucosan record was evaluated using both Microsoft Excel and R. Microsoft Excel was used in an attempt to use sigma values to identify the outliers and to split the record into phases before moving back to R to visualize those phases. All graphs are a result of the R output as are the calculations found in Table 1 and Table 2. In addition to the basic packages allowing for calculation, the gsl and palinsol packages were used to take a closer look at orbital parameters.

### 3.9 Age/depth model

The chronological and stratigraphical ordering of dates allows the levoglucosan data to benefit from an age-depth relationship. Due to ice functioning as a low-interference matrix, aerosol compounds at a range of depths are relatively unaltered resulting in precise dating of the deposition (Gambaro et al., 2008; Blaauw & Christen, 2011). We can depend on the samples closer to the surface to be younger than those at a deeper depth. As a reliable relationship is formed between the depth of the deposit and the age, the paleoclimate can be accurately established and studied (Blaauw & Christen, 2011).

# 4. Results

## 4.1 Statistical analysis of the levoglucosan record

A total of 379 ice core samples from Epica Dome C (EDC) were analyzed. However, within this set of samples 17 of them were below the detection limit and therefore removed from further analysis. Of the 362 remaining ice core samples a range of 1.8 pg $mL^{-1}$ to 430 pg $mL^{-1}$ was detected. In a similar study, analyzing the ice cores from the Talos Dome (TD), the detected range was 4 to 1100 pg $mL^{-1}$ (Battistel et al., 2018). The difference in levoglucosan levels is not a surprise as EDC is an internal site and the transport that occurs in this area differs from that of TD located near the coast and the Ross Ice Shelf. The remote nature of sites located in Antarctica is best shown when compared to sites closer to anthropogenic activity, such as two sites in Tibet that range from 10 ng $mL^{-1}$ to 720 ng $mL^{-1}$ in the Muztagh Ata ice core and 10 ng $mL^{-1}$ to ~100 ng $mL^{-1}$ in the Tangula ice core (Yao et al., 2013).

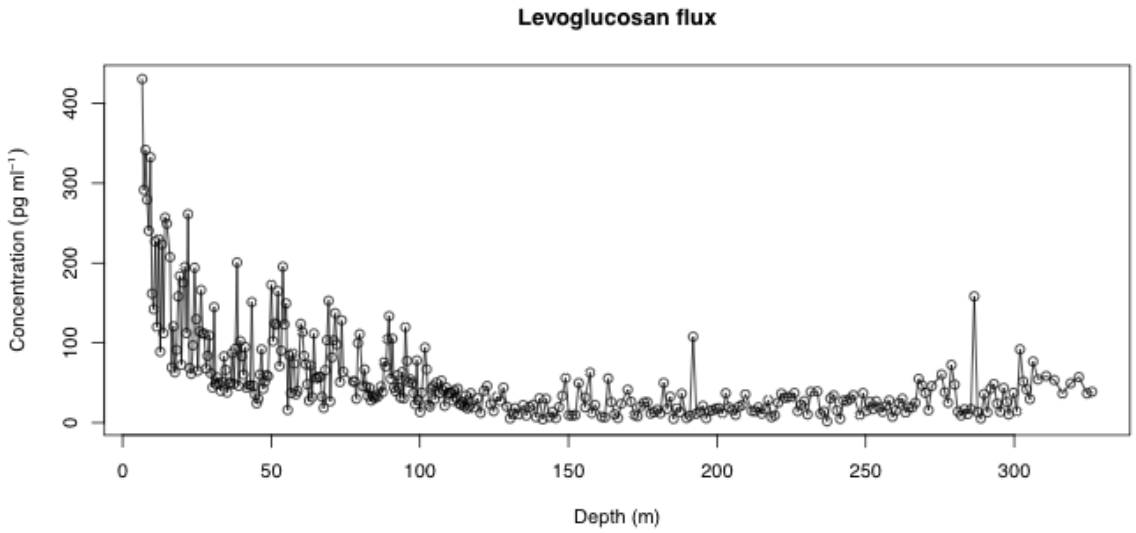


***Figure 4.*** *Levoglucosan concentration data set with no transformations.*

Figure 4 shows the levoglucosan record in the EDC from the mid to late Holocene. All anomalies have been removed from the initial analysis (see Methods). There appears to be less fluctuation between 260 m and 200 m. The shallowest portion of the graph from around 125 m to 6.6 m marks a significant increase of fluctuation and an increase in levoglucosan overall. The spikes on this graph have several different potential explanations such as megafire events, high levels of atmospheric transport, increased level of fire activity,

or simply an error of measurement (Battistel et al., 2018). To better understand the cause of these spikes we must attempt to identify the outliers.

It must be noted that the concentration-depth profile does not significantly differ from the concentration-age record. This correspondence is mainly due to an almost constant accumulation rate in the EDC core section considered in this thesis. Therefore, to better show the results obtained, the levoglucosan records will henceforth be reported and discussed using age, taking advantage of the age-depth model previously mentioned in the Methods section.

Figure 5 shows the levoglucosan record in the EDC from the mid to late Holocene. All anomalies have been removed from the initial analysis (see Methods). As with depth, there appears to be less fluctuation between 8000 yr BP and 6000 yr BP. The youngest portion of the graph from around 3000 yr BP to 0 yr BP marks a significant increase of fluctuation and an increase in levoglucosan overall.

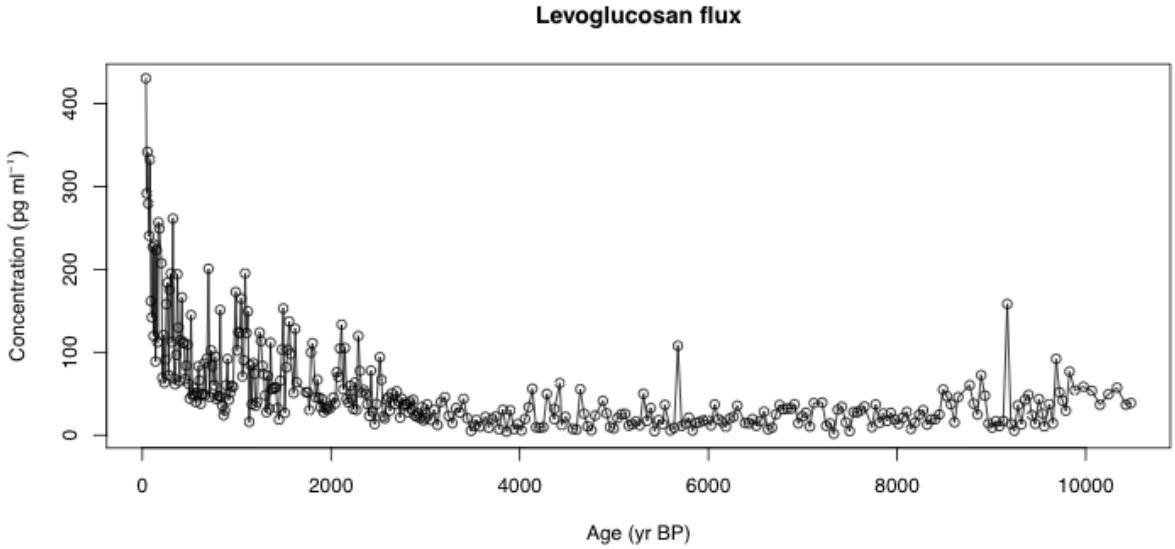


***Figure 5.*** *Levoglucosan concentration data set with no transformations reported in yr BP.*

In order to evaluate the data distribution, a normality test was used. A histogram revealed that the data are not normally distributed. The Shapiro-Wilk test confirmed this occurrence as the p-value is significantly lower than 0.05 and the null hypothesis (i.e. $H_0$ : the distribution is normal) is rejected. Therefore, the data significantly deviates from a normal distribution. A log transformation, as shown in Figure 6a, can be used to ensure the data conforms to a normal or near normal distribution in order to make the data more interpretable. At first glance of the histogram (Figure 6b) the data appears to be more evenly distributed once the data has undergone a log transformation. The Shapiro-Wilk test

confirms this as the p-value is 0.806. As the p-value is above 0.05 the null hypothesis cannot be rejected

(a)

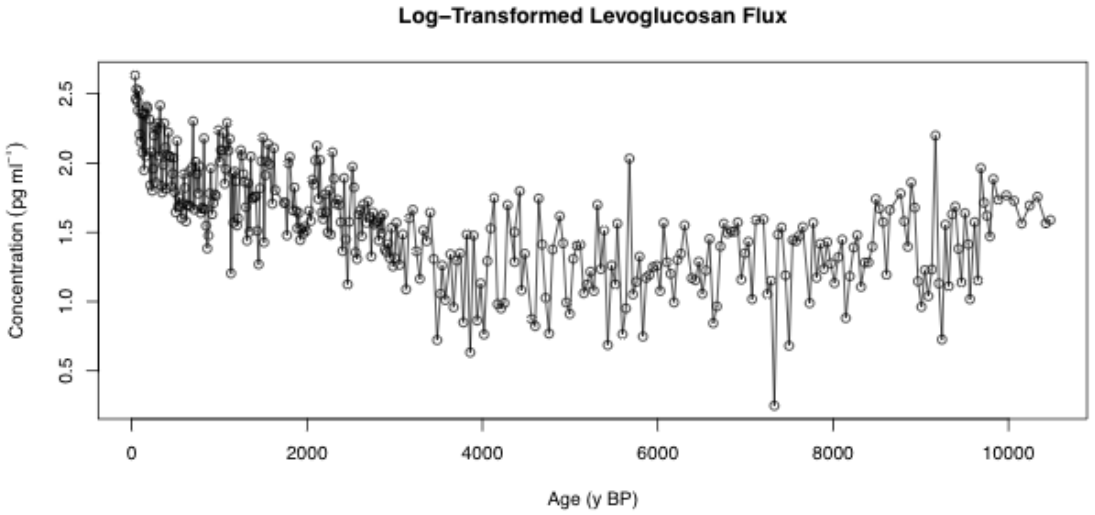


(b)

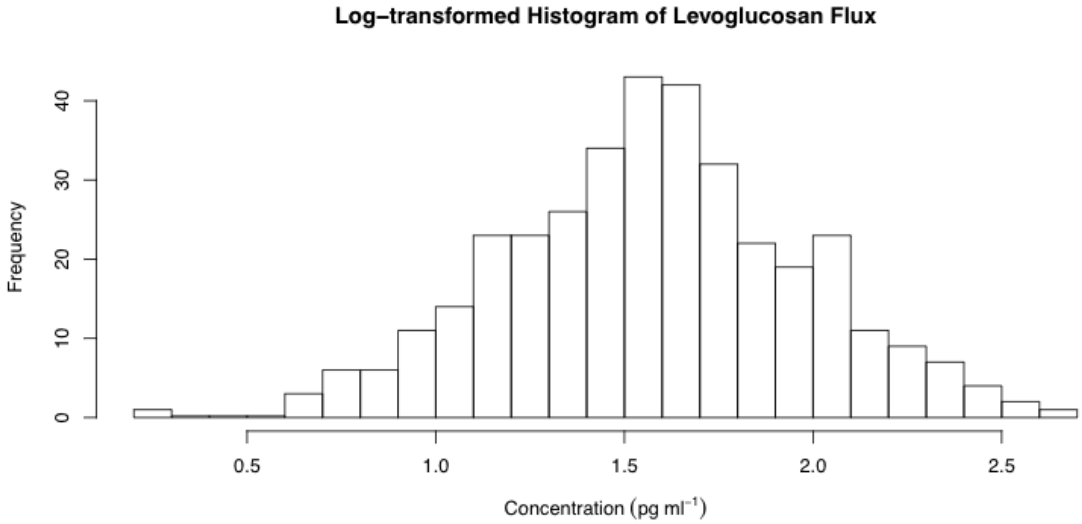


***Figure 6.*** *(a) Levoglucosan record with no anomalies and having undergone a log transformation. (b) Histogram of log-transformed levoglucosan record.*

In order to smooth the record and potentially identify outliers, a local polynomial regression, LOESS, can be used. Span parameters control the fit at a specific point in the series and then weights the data nearest to it. The span parameters were altered several times to find the best conditions. Ultimately, in order to capture more trends, a span of .2 was used (Figure 7a), and to smooth the fit more and show a comparison, a span of .75 was also used (Figure 7b).

(a)

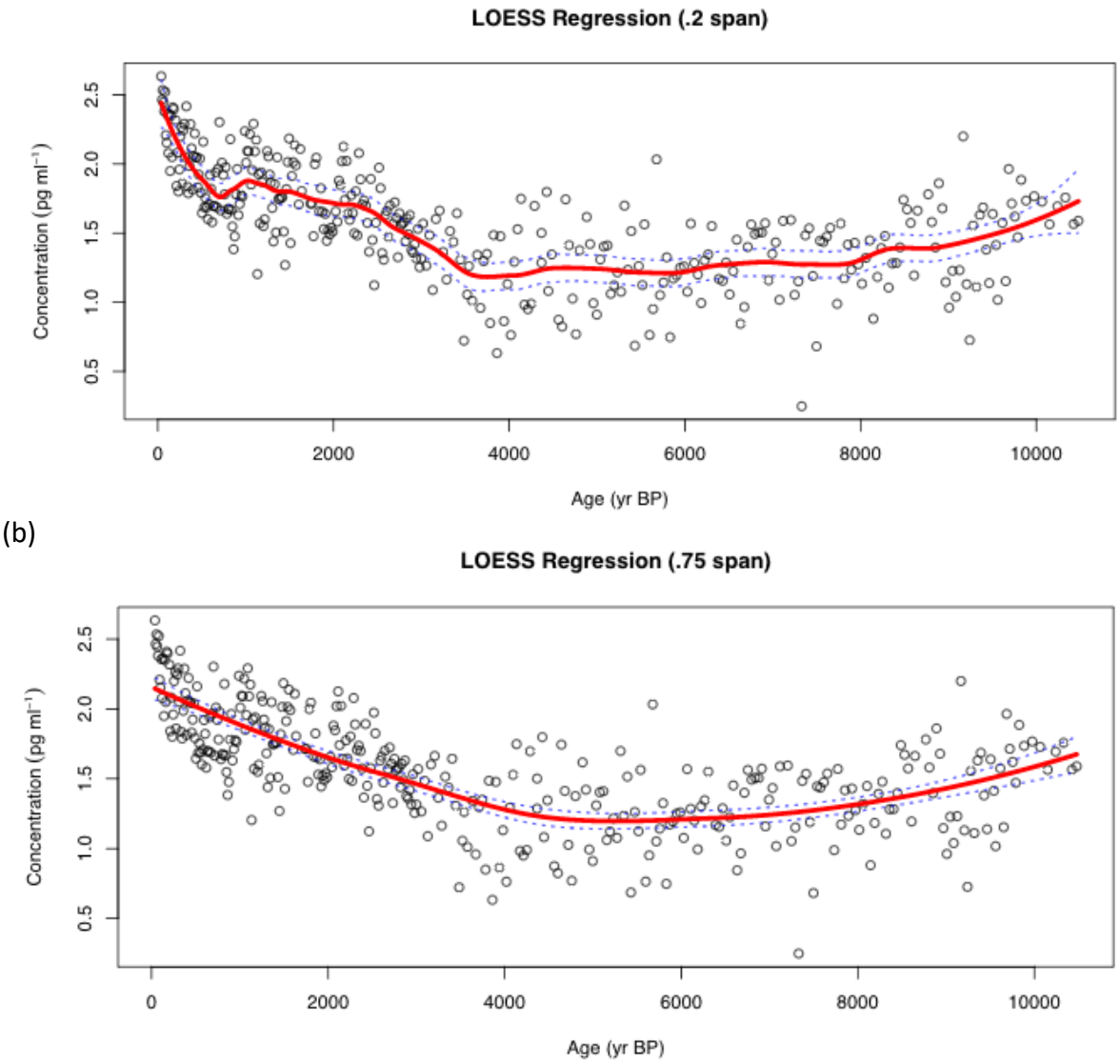


***Figure 7.*** *(a) LOESS regression using .2 as the span parameter and concentration as the target variable. (b) LOESS regression using .75 as the span parameter and concentration as the target variable.*

In both examples the confidence band is not robust enough to fully capture the temporal trends. As a result, we are limited by LOESS as it is not representative and leaves too many outliers to truly be an effective statistic tool.

A second attempt at separating the outliers from the potential megafire events, lies within using the standard deviation and the amount of sigma values with respect to the mean, based on the approach proposed by Zennaro et al. 2015. Here, however, we don't calculate the standard deviation of the overall record but calculate the standard deviations and the mean of the *n* nearest neighbours of the suspected value. The latter approach was preferred as it seems to better recognize anomalous values, especially in the oldest part of the record where higher levoglucosan concentrations significantly exceed the neighbors but are

comparable with most of the values observed in the more recent part of the record. If the suspected value exceeds three times the standard deviation, it was considered a potential megafire event. The numbers of the nearest neighbours considered was *n*=2 (one left and one right, criterion I) and *n*=4 (2 left and 2 right, criterion II). The amount of potential megafire events differs depending on the selected criteria, but in both attempts the megafires outnumbered the outliers. The first attempt (criterion I) showed 33 outliers and 59 megafires (Figure 8a). The second (criterion II) showed 7 outliers and 23 megafire events (Figure 8b).

(a)

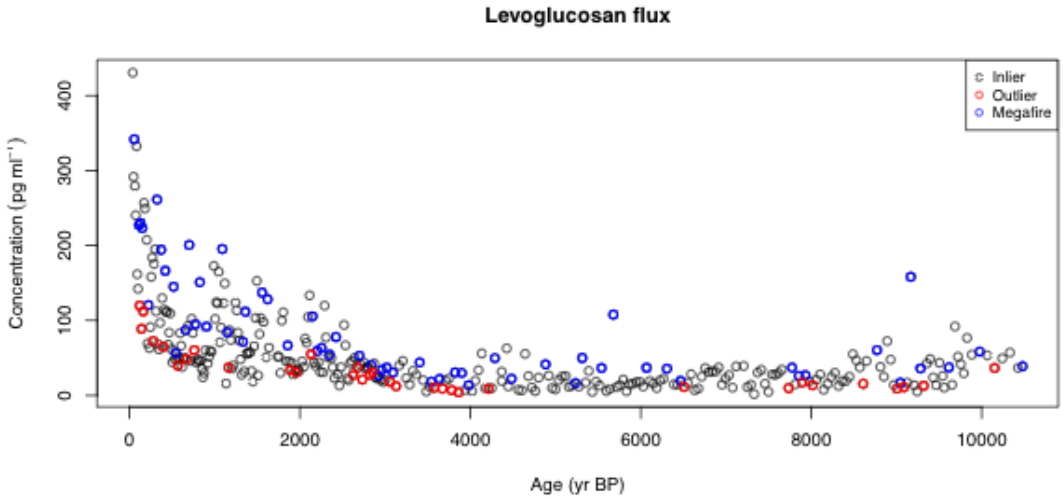


(b)

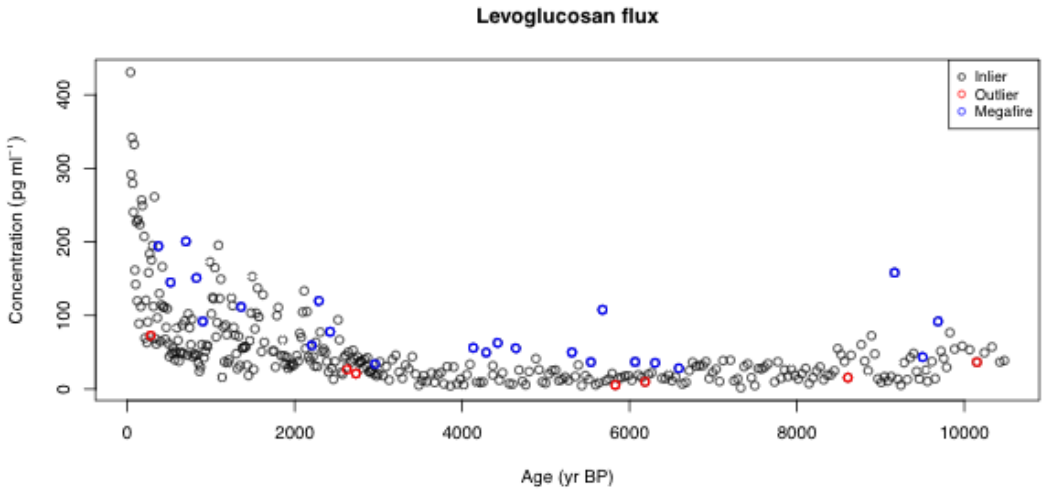


***Figure 8.*** *(a) Levoglucosan concentration with potential outliers and megafires calculated using criterion (I). (b) Levoglucosan concentration with potential outliers and megafires calculated using criterion (II).*

The potential megafires appear to increase in number as the levoglucosan fluctuation increases, with the largest number occurring in the earliest part of the record (3000 yr BP – present) which is also the time period with the most significant increase.

### 4.2 Charcoal Synthesis

To reconstruct the fire history in a more global manner, we can turn towards the synthesis of charcoal records (Marlon et al., 2013). Synthesizing these charcoal records and comparing them to the levoglucosan record can allow us to observe the long-term trends in fire activity and changes of burning biomass patterns of regions located near Antarctica (Battistel, 2018). It must be noted that there is a large amount of speculation involved when using the individual spikes in the charcoal record to validate individual spikes in the levoglucosan record (Battistel, 2018). For example, a study conducted by Iglesias & Whitlock (2014) revealed high charcoal signals in Laguna Huala Hué, Argentina (GCD code: 1140) between roughly 800 yr BP – present. This is consistent with high charcoal signals in records between roughly 600 yr BP – 100 yr BP analyzed by Mariani & Fletcher (2017) from Hartz Lake, Australia (GCD code: 1213). While this correlation could be valuable, the peaks also may indicate a short period of efficient transport or intense local fire events (Battistel, 2018).
In order to get a better indication of transport and to see the potential for correlation, charcoal records were chosen from four areas: the Southern Hemisphere between 90 and 30°S, southern South America between 90 and 30° S and between 60 and 80°W, southern Africa between 90°S and 0° and between 0° and 70°E, and Australia/New Zealand between 90 and 30°S and between 140 and 180°E (Figure 9). These records underwent a three-step transformation in preparation for the comparison with the levoglucosan records (Blarquez et al., 2014). First the data undergoes a min-max rescaling, next a Box-Cox transformation to ensure variance homogenization, and finally rescaling the data to obtain Z-scores (Blarquez et al., 2014).

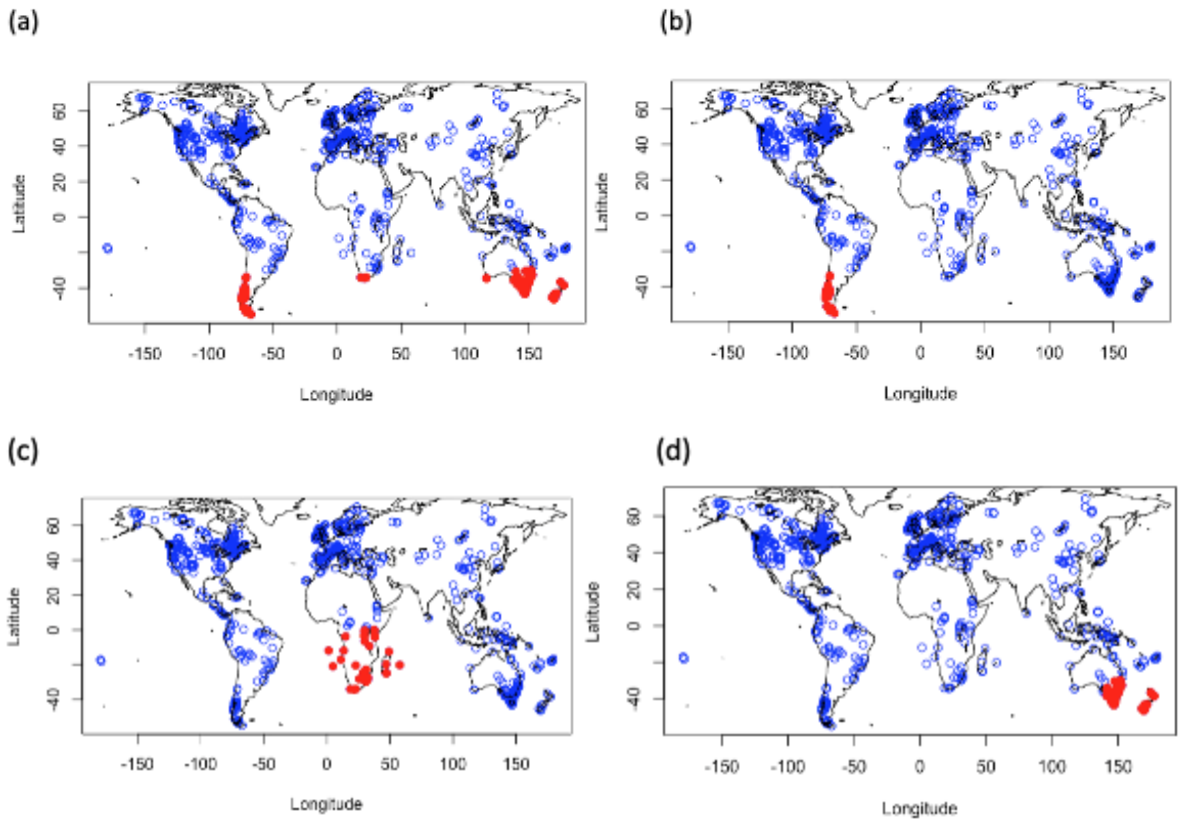


***Figure 9.*** *Charcoal synthesis of (a) Southern Hemisphere, (b) South America, (c) Africa, (d) Australia and New Zealand. Blue circles represent unselected GCD sites, and red dots represent the selected sites.*

By splitting the levoglucosan and charcoal records into 500, 200, 100, 50, and 25 year intervals, temporal patterns of fire events can be better analyzed. In evaluation of the relationship between the variables of charcoal and levoglucosan, a simple linear regression model was used. In this case the explanatory variable is levoglucosan and the response variable is charcoal

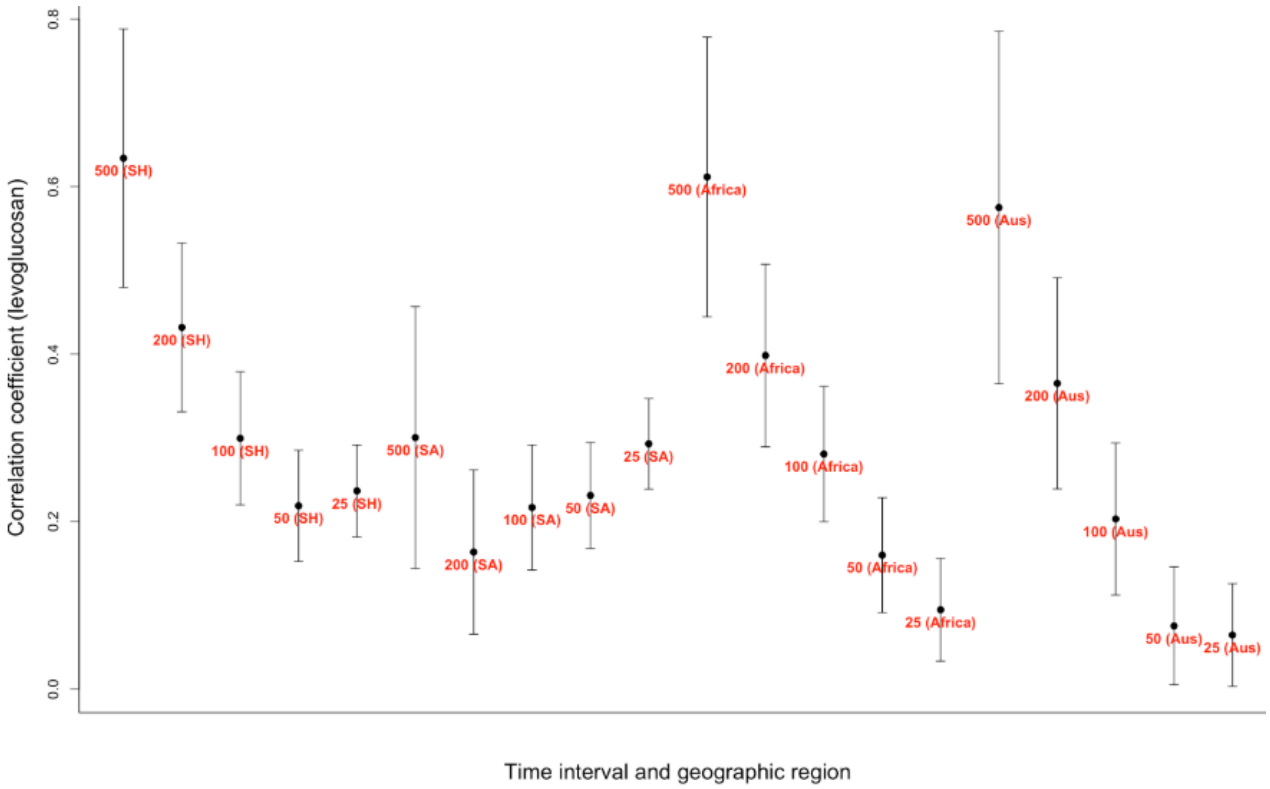


***Figure 10.*** *The correlation between levoglucosan recorded at EDC and the charcoal synthesis from the Southern Hemisphere (SH), South America (SA), Africa, and Australia/New Zealand (Aus).*

When observing the output of the linear regression, attention can be brought to two statistical values, r, the correlation coefficient (Figure 10), and the p-value (Table 2). These statistical values work together. If the p-value is less than 0.05, the correlation is considered significant. The correlation coefficient itself, which measures the strength and direction of a linear relationship between charcoal and levoglucosan within the records, is positive in each of the five intervals and four regions indicating a positive linear relationship. The strength of this relationship differs and drops as we move through the different intervals. The 500-year interval has the strongest linear relationship in each sampled region.

***Table 2.*** *Correlation coefficient through the five selected time intervals of the Southern Hemisphere, South America, Africa, and Australia/New Zealand. The p-value is based on the usual significance level, alpha = 0.05. If the p-value is <0.05 (red), the correlation is considered significant. If the p-value is >0.05 (black), the correlation is not considered significant.*

| | Nr. Sites | 500 yr | 200 yr | 100 yr | 50 yr | 25 yr |
|---|---|---|---|---|---|---|
| Southern Hemisphere | 183 | 0.634 | 0.432 | 0.300 | 0.219 | 0.237 |
| South America | 32 | 0.300 | 0.164 | 0.217 | 0.231 | 0.293 |
| Africa | 35 | 0.612 | 0.398 | 0.281 | 0.160 | 0.095 |
| Australia and New Zealand | 142 | 0.575 | 0.365 | 0.203 | 0.075 | 0.064 |

### 4.3 Identification of phases

After studying the temporal trend, the record was split into seven phases (Figure 11a-g) to better evaluate the potential transitions in fire regimes.

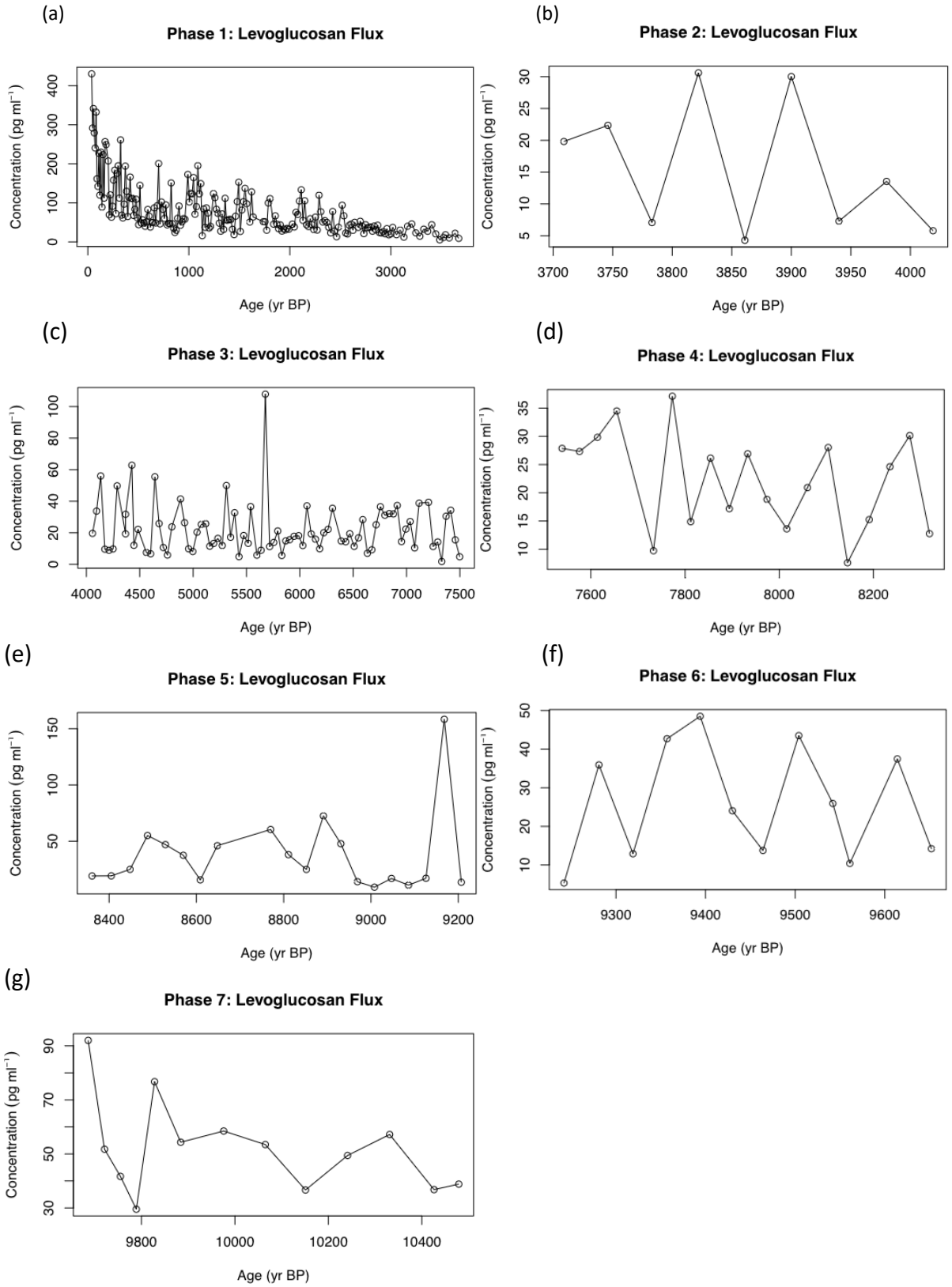


***Figure 11.*** *The seven phases of the levoglucosan flux. Please note the changes in the axes. (a) Phase 1 of the levoglucosan record spanning from 38 yr BP to 3672 yr BP. (b) Phase 2 of the levoglucosan record spanning from 3709 yr BP to 4019 yr BP. (c) Phase 3 of the levoglucosan record spanning from 4057 yr BP to 7498 yr BP. (d) Phase 4 of the levoglucosan record spanning from 7539 yr BP to 8319 yr BP. (e) Phase 5 of the levoglucosan record spanning from 8361 yr BP to 9207 yr BP. (f) Phase 6 of the levoglucosan record spanning from 9242 yr BP to 9652 yr BP. (g) Phase 7 of the levoglucosan record spanning from 9686 yr BP to 10479 yr BP.*

To ensure that the data sets are normally distributed within the phases, a histogram and Shapiro-Wilk test were utilized. According to the histograms and the p-value calculated for each section, several phases were already considered to have a normal distribution. As a result, no log transformation was completed, and the following analysis was conducted under the assumption of normality.

To determine if the sample means are significantly different between the phases, 21 Welch Two Sample t-tests were conducted (Table 3). If the p-value was less than .05, the null hypothesis was rejected and there does appear to be a difference between the averages of the two groups. If the p-value was greater than .05, there was a failure to reject the null hypothesis.

***Table 3.*** *Welch Two Sample t-test results based on the usual significance level, alpha = 0.05. If the test is considered statistically different (red), there is a difference between the true averages. If the test is not statistically different (black), there is no difference between the true averages.*

| Phase | 1 | 2 | 3 | 4 | 5 | 6 | 7 |
|---|---|---|---|---|---|---|---|
| 1 | - | 8.479e-16 | 2.2e-16 | 2.2e-16 | 2.789e-05 | 3.802e-11 | 0.0001 |
| 2 | - | - | 0.1142 | 0.1189 | 0.0151 | 0.0712 | 5.201e-06 |
| 3 | - | - | - | 0.9929 | 0.0655 | 0.4082 | 2.749e-05 |
| 4 | - | - | - | - | 0.0670 | 0.4172 | 2.776e-05 |
| 5 | - | - | - | - | - | 0.2112 | 0.1121 |
| 6 | - | - | - | - | - | - | 0.0005 |
| 7 | - | - | - | - | - | - | - |

A boxplot can help to better compare the distributions between the phases (Figure 12). A large number of outliers can be observed in phase 1, while outliers are absent from phases 2, 4, and 6.

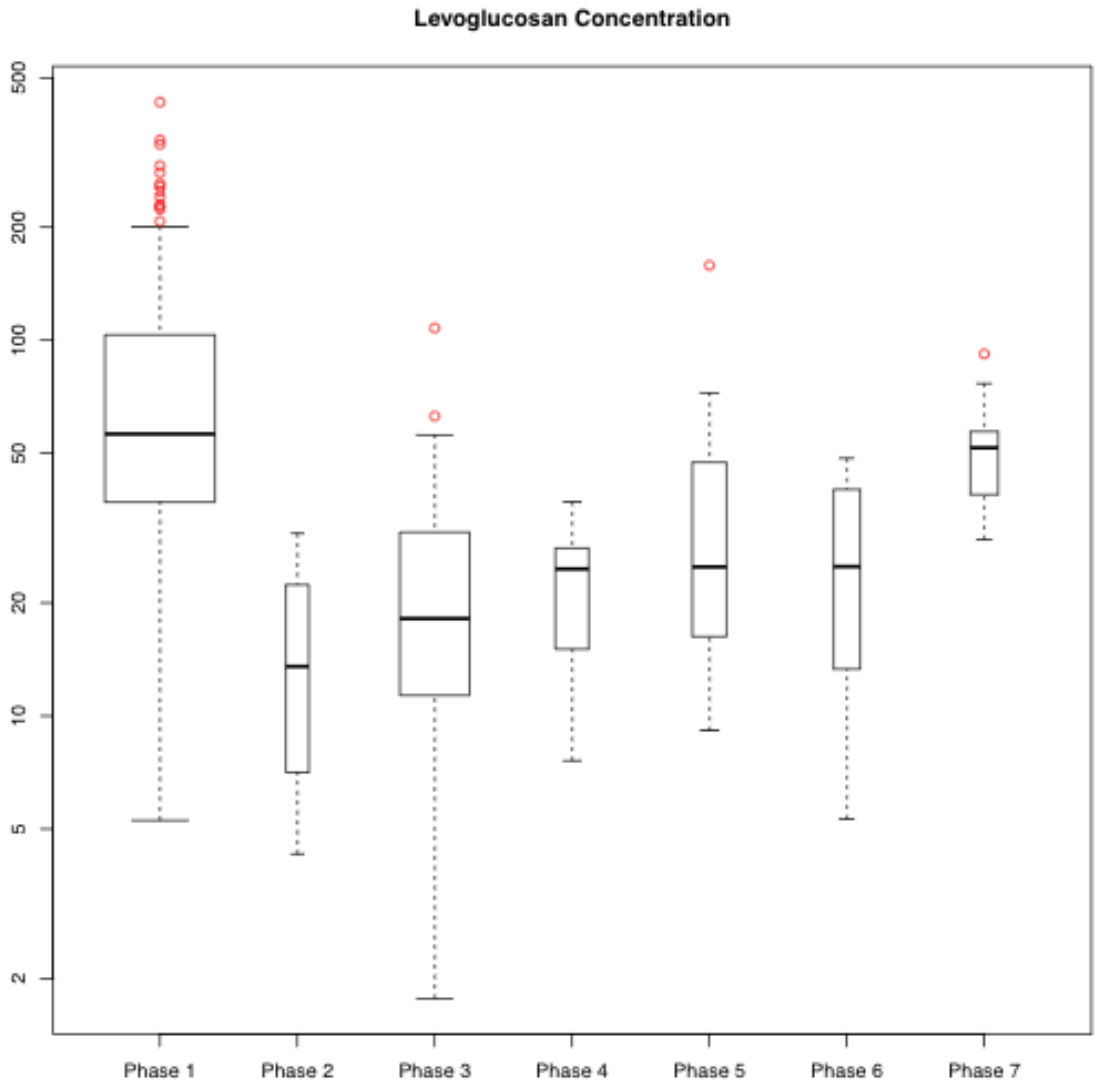


***Figure 12.*** *Phase 1 of the levoglucosan record spanning from 38 yr BP to 3672 yr BP. Phase 2 of the levoglucosan record spanning from 3709 yr BP to 4019 yr BP. Phase 3 of the levoglucosan record spanning from 4057 yr BP to 7498 yr BP. Phase 4 of the levoglucosan record spanning from 7539 yr BP to 8319 yr BP. Phase 5 of the levoglucosan record spanning from 8361 yr BP to 9207 yr BP. Phase 6 of the levoglucosan record spanning from 9242 yr BP to 9652 yr BP. Phase 7 of the levoglucosan record spanning from 9686 yr BP to 10479 yr BP.*

# 5. Discussion

## 5.1 Atmospheric Transport

Using back trajectory, a method of analysis that traces a parcel of air from the location it was sampled back to its origin, we are able to determine the potential source contributions of biomass burning emissions. However, it is not clear that atmospheric transport of today was constant throughout the Holocene. According to a study by Stohl and Sodemann (2010), the subpolar band located around Antarctica has the lowest probability for transport from the stratosphere at any time of the year. However, as seen in Figure 13, Antarctica's interior has a much higher transport probability than the subpolar band (Stohl and Sodemann, 2010). This is due to the subsidence over Antarctica as well as stratospheric intrusions that happen within midlatitude cyclones (Stohl and Sodemann, 2010).

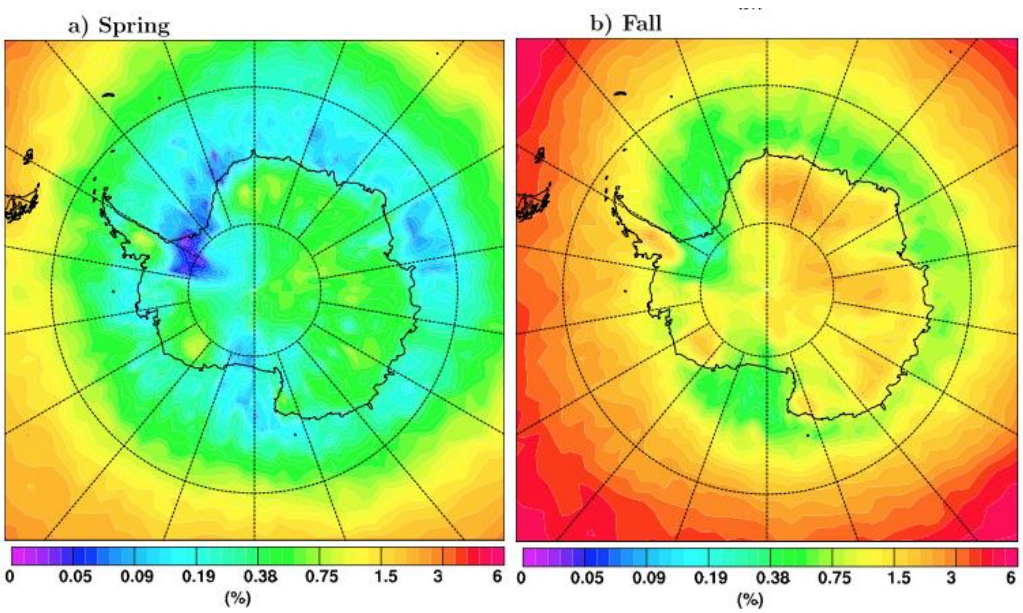


***Figure 13.*** *Probability that within the last 10 days air has arrived from the stratosphere and entered the lowest 500 m in both spring and fall. Spring is defined as September, October, and November and fall is defined as March, April, and May. Stohl and Sodemann (2010).*

To determine potential sources of levoglucosan the time of year must be taken into consideration as South America and Australia reach a maximum of biomass burning in the spring, and Southern Africa reaches a maximum during the winter.

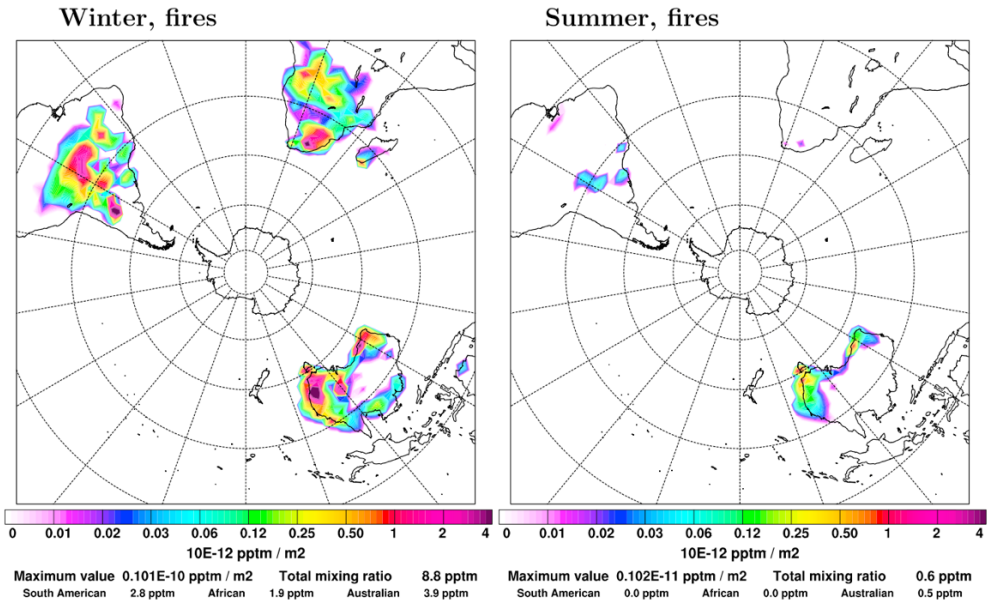


***Figure 14.*** *Potential source contributions of black carbon from biomass burning in both winter and summer. The particles had to spend a minimum of five days in the Antarctic and reach an altitude of at least 1000 m above sea level. Stohl and Sodemann (2010).*

In a study conducted by Hu et al. (2013), Levoglucosan was detected in a sample recovered from 62.21°S, 97.77°E. The back trajectory determined that this levoglucosan had been transported by westerly winds from West Antarctica (Hu et al., 2013). At another site in which levoglucosan was detected, located at 66.40°S, 68.39°E, it would have to be transported over continental Antarctica by easterly winds as it is south of the ACT (Hu et al., 2013). As the surface inversion is weaker and there is a breakdown of the circumpolar vortex in the summer, South America is the likely origin point in both of the aforementioned samples (Hu et al., 2013). Because the levoglucosan found at 66.40°S, 68.39°E would have been transported over continental Antarctica, Hu et al. hypothesized that levoglucosan would have been deposited in continental Antarctica in higher detectable levels (2013). The ice cores collected from EDC support their hypothesis.

## 5.2 Vegetation during the Holocene

Biomes and ecosystems continue to shift as the climate shifts. As a result, the biomes and vegetation patterns we see today are not completely consistent with the biomes and vegetation patterns present during the Holocene, as seen in Figure 15.

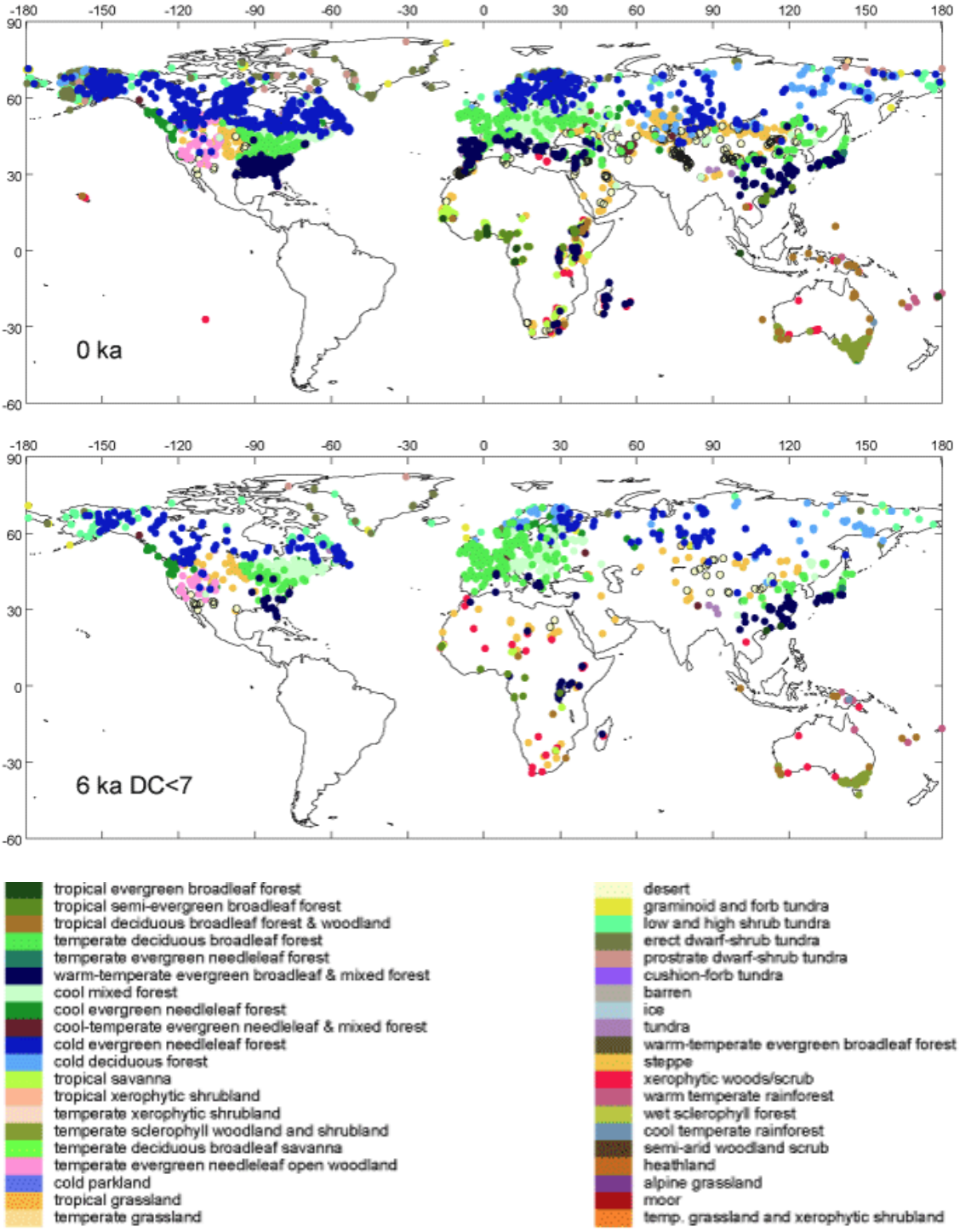


***Figure 15.*** *Vegetation maps produced by BIOME 6000 comparing the vegetation patterns from 0 ka and 6 ka. Harrison and Prentice (2003).*

Before satellite records came into existence, our understanding of varying biomes, and specifically grasslands, is relatively limited (Berangere et al., 2018). In order to better understand global biomass burning and the resulting emissions, we must consider the differences in not only the continents, but between grasslands and forests as well (Berangere et al., 2018).

### 5.3 Climatic Variables

Levoglucosan signals are not just subject to atmospheric transport nor is their occurrence limited to the availability of biomass. While those are two important variables, as without biomass to be burned and without transport to Antarctica there would be no levoglucosan to be found, we must consider other variables that can limit or enhance the burning of biomass. Each variable could cause the levels of levoglucosan to be misrepresented whether it be by making a fire event seem more extreme, or by limiting transport and thereby eliminating the fire record. Some of these variables are temperature, precipitation-evaporation cycle, ENSO, SAM, orbital parameters, as well as the seasonal insolation. Other variables such as $CH_4$ or $CO_2$ help to provide context to the levoglucosan record.
In the last ~200 kyr the atmospheric concentration of $CH_4$ (methane) has shifted considerably (Bender et al., 2007). While wildfires are not the top driver of methane emissions (Table 3) changes in the fire regime and biomes during the Holocene help substantiate the changes in the $CH_4$ record (Chappellaz et al., 1993, Bock et al., 2017).

***Table 4.*** *Natural budgets of methane throughout the Last Glacial Maximum, Pre-industrial Holocene, and up to 1993. Chappellaz et al. (1993).*

| Source/sink | Present* | Preindustrial Holocene | LGM |
|---|---|---|---|
| wetlands | 115 | 135 | 75 |
| wild animals | 2–6 | 15 | 20 |
| termites | 20 | 20 | 20 |
| wildfires | 5 | 5 | 5 |
| ocean/freshwater | 10 | 10 | 10 |
| $CH_4$ hydrates | 5 | 5 | 0 |
| soil sink | −10 | −10 | −10 |
| total | 150 | 180 | 120 |

Methane serves as a climate proxy that, according to Bender et al. (1997), best interprets changes such as precipitation or temperature. However, in a study conducted by Bock et al. (2017), methane that is enriched in $^{13}C$ ($\delta^{13}CH_4$), is sourced from geologic emissions of old methane as well as burning biomass (2017). While the Holocene is the time period under observation, it is of interest to expand the time period when considering methane in order to see the increase of $\delta^{13}CH_4$ emissions leading up to the Holocene as seen in Figure 16 (Bock et al., 2017).

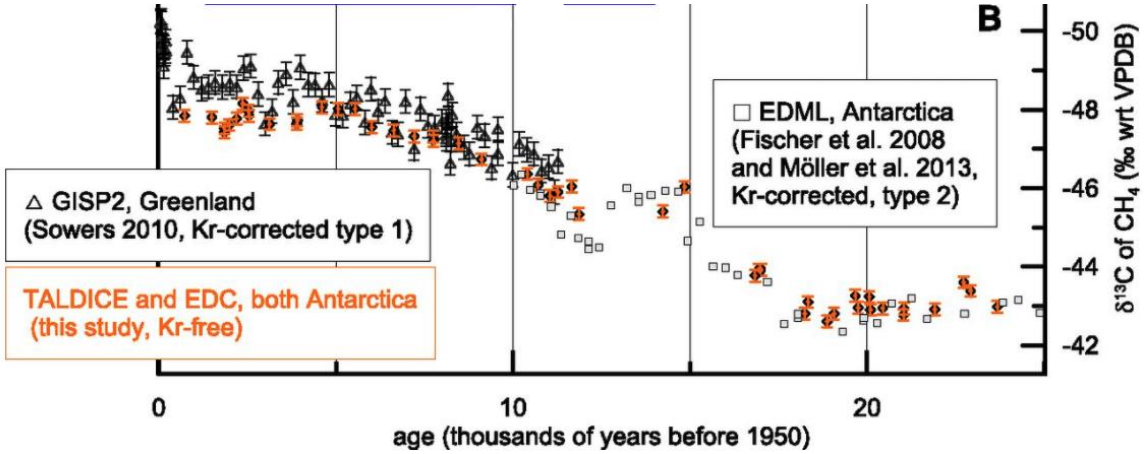


***Figure 16.*** *Methane ($\delta^{13}CH_4$) levels from GISP2 in Greenland, TALDICE, EDML, and EDC in Antarctica. These records have been measured with no krypton interference. Bock et al. (2017).*

Decreasing $CH_4$ emissions are observed as peatlands change into bogs which helps to explain why $\delta^{13}CH_4$ emissions began to level out throughout the Holocene. However, the biomes alone cannot account for the increase as observed in Figure 16 (Bock et al., 2013). In the study that Bock et al. (2017) oversaw, an increase in fire frequency due to the decrease in herbivorous megafauna is a likely culprit of the extreme changes. In fact, by using the $^{13}C$ isotope, Bock et al.'s (2017) study found that the Holocene was impacted by a higher level of fire activity when compared to the Last Glacial Maximum.

Variations in the fire activity are impacted by several different drivers with temperature classified as the most important (Battistel et al.,2018). However, temperature is not the variable that fire is directly dependent on, and there is not a direct linear relationship between the two (Battistel et al., 2018). Temperature is responsible for influencing and driving fire-supporting weather (Daniau et al., 2012). Temperature does play a large role in the precipitation - evaporation balance which is considered the second most important driver related to fire activity (Daniau et al., 2012; Battistel et al., 2018). This cycle, or balance, works to explain the amount of fuel available to burn in different environments (Daniau et al., 2012). The key to higher fire activity and greater amounts of burning biomass lies within an environment experiencing intermediate moisture levels (Daniau et al, 2012). If the environment is already considered wet and it experiences an increase in precipitation, the increase in available precipitation to burn is offset by the fuel being too wet to burn (Daniau et al, 2012). If what is considered to be a dry environment sees an increase in precipitation, there will be more vegetation available to burn and in turn, more fire activity (Daniau et al, 2012).

Despite an irregular two-to-seven-year pattern, the disruptions in precipitation, temperature, wind, and atmospheric transport that happen during El Niño and La Niña (ENSO) are fairly predictable (Muñoz-Díaz et al., 2005). While changes in precipitation and temperature affect the biomass that is available for fuel, changes in geopotential height (Figure 17) affect the pressure surface and therefore affect the atmospheric transport over Antarctica (Markle et al., 2012).

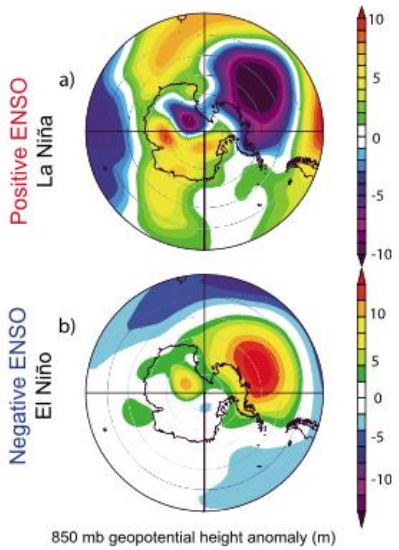


***Figure 17.*** *a) Geopotential height anomalies that occur during a) La Niña and b) El Niño. Markle et al. (2012).*

Whether it is a typical or ENSO year, cyclonic flow originates from one of two climatologically low-pressure areas, Amundsen Sea or Ross Sea effecting West Antarctica (Markle et al., 2012). East Antarctica tends to experience more anti-cyclonic and trans-continental flow (Markle et al., 2012). The geopotential heights shift according to the positivity or negativity of the ENSO with positive anomalies being associated with a negative ENSO and an increase in Amundsen Sea trajectories, and negative anomalies associated with a positive ENSO and an increase in Ross Sea trajectories (Markle et al., 2012). As EDC is located in Eastern Antarctica, La Niña events (positive ENSO) are of particular interest because there is an increase in trajectories that cross West Antarctica as the low-pressure system in the Amundsen Sea is stronger (Markle et al., 2012).

Roughly 35% of climate variability in the Southern Hemisphere can be attributed to the Southern Hemisphere Annular Mode, otherwise known as SAM (Marshall, 2007). Gong and Wang (1999) proposed an empirical definition to calculate SAM, it is the difference in zonal

mean atmospheric pressure at 40° and 65°S. Much like ENSO, the conditions in different parts of Antarctica react differently to positive or negative SAM values (Marshall & Thompson, 2016). If SAM is positive West Antarctica will experience wet conditions and East Antarctica will experience drier conditions as seen in Figure 18 (Marshall & Thompson, 2016).

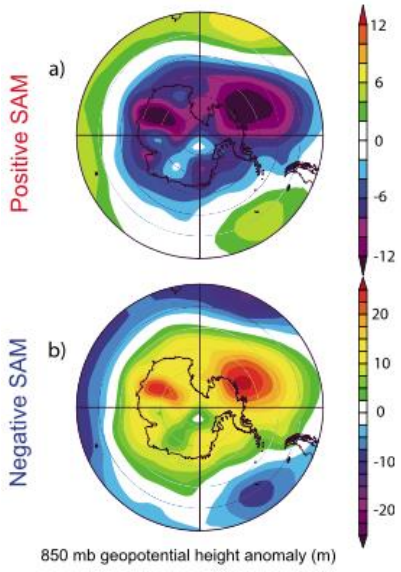


***Figure 18.*** *a) Geopotential height anomalies that occur during a) Positive SAM and b) Negative SAM. Markle et al. (2012).*

The wet conditions experienced in Western Antarctica during a positive SAM extend to South America which endures a southward shift of storms, which may lead to an increase in aerosol transport (Battistel et al., 2018). In a study conducted by Gomez et al. (2011), stable isotope temperature estimates for the EPICA Dome C ice core were used to attempt to link SAM to long-term temperature changes. However, the results indicate that annual insolation and precession have a greater impact (Gomez et al., 2011).

The amount of solar radiation that a planet receives is called insolation. Insolation, much like temperature, is a major driver of biomass burning (Zennaro et al., 2015). While insolation alone does not cause fire, there does tend to be a correlation of insolation and fire activity (Zennaro et al., 2015). This is due to insolation affecting the growth of vegetation (Battistel et al., 2018).

### 5.4 Orbital Parameters

A study by Arienzo et al. (2017) considered South America to be the dominant source of black carbon in Antarctica and it is postulated that these changes are in part linked to

insolation. To greater understand insolation patterns affecting the Southern Hemisphere, it is useful to take a closer look at the Milankovitch cycles: obliquity, eccentricity, and precession (Campisano, 2012). Affecting the distribution of solar radiation is obliquity (Timmerman et al., 2014). As the Earth moves through high and low obliquity phases, the annual mean insolation varies (Figure 16a) (Timmerman et al., 2014). Earth's orbit is not a perfect circle, eccentricity measures the shape of Earth's orbit, and how elliptical it is (Buis, 2021). According to NASA Earth's eccentricity is small and therefore its effect on insolation is negligible (Figure 16b) (Buis, 2021). The sun and the moon are gravitational influences upon Earth, these influences cause Earth to totter on its axis as it rotates and as it orbits (Buis, 2021). This precession cycle causes the differences in how both hemispheres experience their seasons (Figure 16c) (Buis, 2021). As this cycle is 25,771.5 years long, and we have 13,000 years until the conditions flip, we can assume that present-day seasons are similar as to the seasons in the Holocene (Buis, 2021). The Southern Hemisphere experiences more extremes in solar radiation, hot summers, and little moderation between seasons (Buis, 2021). As can be seen in all three of the orbital parameters, the cycle is long and gradual enough to not have a significant impact on the levoglucosan increase that is observed in the early (3000 yr BP-present) Holocene.

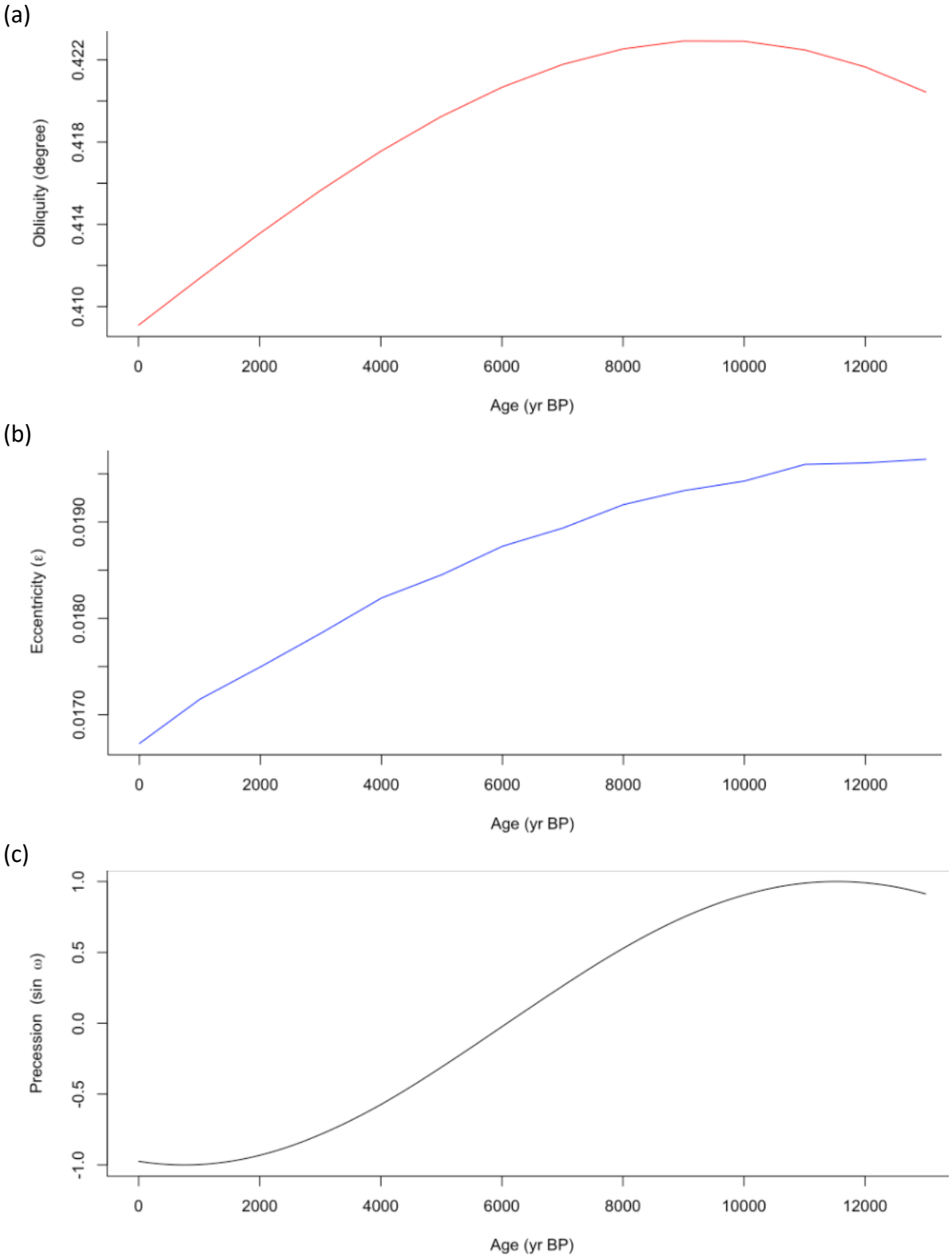


***Figure 19.*** *Orbital parameters a) obliquity, b) eccentricity, and c) precession throughout the Holocene.*

### 5.5 Charcoal correlation

The analysis and results above appear to indicate an increase in anthropogenic activity which led to an increase in the burning of biomass during the more recent years. This could be due to an increase in agriculture throughout the Holocene. Agriculture is an intensive resource-use system, and its evolution would have been relatively slow (Richerson et al., 2001). The development of agriculture impact would be sparce in the beginning, but with an increase in population and land use, this evolution became exponential not linear as can be seen in the levoglucosan flux (Figure 5) and as will be discussed.

The evidence of correlation between charcoal and levoglucosan is strongest in the Southern Hemisphere and weaker from individual regions with the exception of Africa which shows a strong correlation, but a limited number of sites (Table 2). Within the Southern Hemisphere the correlation appears to increase when the window of time is larger (i.e., 500-year time interval is higher than the 25-year time interval). This means that the levoglucosan from EDC better intercepts the long-term variations rather than the short-term variations. Overall, the correlation is higher within the Southern Hemisphere, suggesting that EDC is able to collect a hemispheric signature of fires, and indicates a natural synthesis and evolution of fire occurrence in the Southern Hemispheric level as a whole.

### 5.6 Levoglucosan phases

We can observe that Phase 7 (9700 yr BP to 10500 yr BP) is statistically different from the other phases. This is partly because when the Holocene started fire activity was high, due to the movement from glacial to interglacial (Marlon et al., 2013). At this time $CO_2$ and temperature increased causing the biomass to flourish. The temperature record as seen in Figure 20 helps support this as the temperature gradient changed abruptly. This rate of change is important as it is a natural factor that strongly effects fire occurrence as can be noted in the early Holocene (Battistel et al., 2018). It is likely that wet and dry seasons began to alternate at this time which promoted fire activity. Moreover, monsoons reached their maximum about 8,000 yr BP and this played a role in creating wet summers (more biomass) followed by more arid mid-seasons. During the mid-late Holocene, temperature slowly decreased likely impacting fire activity. This is evident in the box plot (Figure 12) as there is a slow and progressive decrease in the mean from Phase 7 to Phase 2. Phase 2 is not

different from its adjacent Phase 3 or even Phase 4, but it is different from Phase 7. If only natural factors are assumed, the results indicated in Phase 1 would be unexpected. It is logical to assume that the signal present in Phase 1 can be deemed anthropogenic.

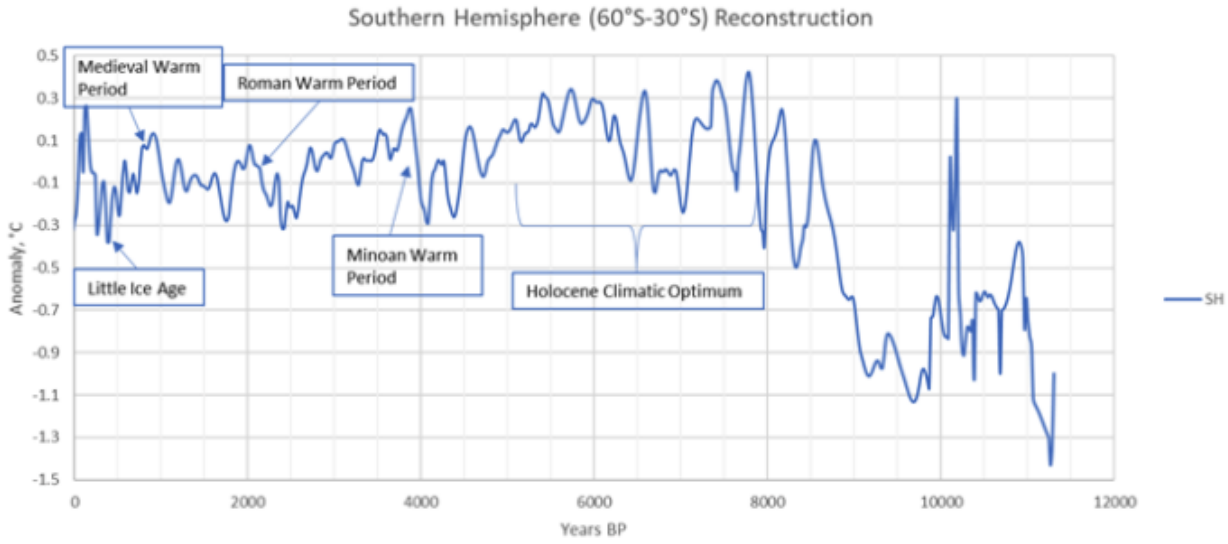


***Figure 20.*** *Temperature anomalies between 60°S-30°S. May (2017).*

The rate of change in regard to the temperature is lower in the late Holocene. In fact, the natural climate as a whole did not experience much natural variability in the late Holocene (Battistel et al., 2018). Therefore, it is logical to assume the signal observed in Phase 1 (40 yr BP to 3700 yr BP) could be anthropogenic. This increase, that begins between 4000-3000 yr BP, could be attributed to the impact of early human activities such as agriculture. This is shown further in Table 3, as it appears the fire regime began to move away from a natural stability. This could be a result of anthropogenic influence as humans made a move towards agriculture. According to a study conducted by Stephens et al., land use increases for the purpose of intensive agriculture can be dated to roughly 3000 years BP at a global level (Figure 18) (2019).

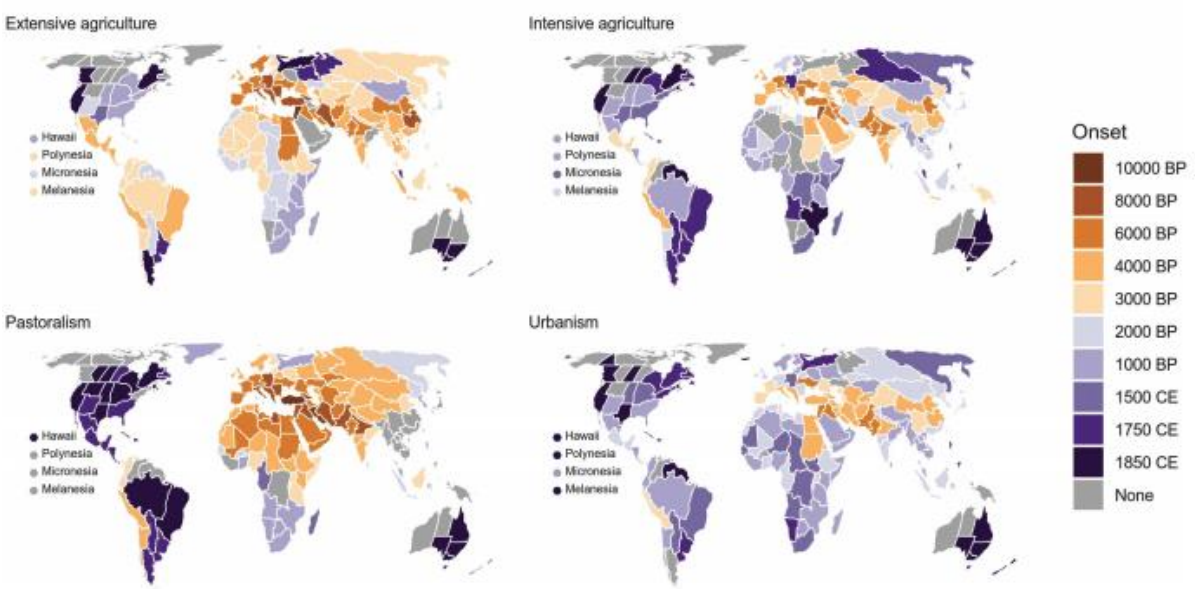


***Figure 21.*** *Earliest agriculture onset at the common prevalence level which is 1-20% of the land area. Stephens et al. (2019).*

As can be noted by Figure 21, the Southern Hemisphere experience delayed and limited development of agriculture when compared to the Northern Hemisphere (Battistel et al., 2018). However, Richerson et al. (2001), argues that the use of agriculture would help groups out-compete the groups that relied upon hunting and foraging. Therefore, during the Holocene, the Southern Hemisphere would be impacted by a constant move towards subsistence intensification (Richerson et al., 2001).

## 6. Conclusion

In this thesis, I evaluated the levoglucosan record obtained from the analysis of the EDC ice core collected in Antarctica when the site was actively being drilled from 1993-2004. The analysis of the record and the comparison with the major climatic variables show that the fire regime abruptly increased during the early Holocene mainly due to the abrupt transition from the glacial to the interglacial period. The increase during the Holocene is consistent with the contribution of natural factors as an increase in temperature affected the biomass availability and promoted the oscillations between seasonal wet and dry conditions. It is likely that the high monsoon activity during the early Holocene may have played a role in enhancing fire activity. During the mid-Holocene, the decrease in monsoons as well as the stabilization of the climate may have contributed to a reduction in the fire occurrence. Finally, around 3500 yr BP, fire increased to values even higher than during the Early Holocene. This increase is quite unexpected since natural factors did not fully corroborate the increase. This change in fire regime is therefore more likely due to anthropogenic factors that are related to an increase or intensification of the agricultural activity required to create open spaces or from taking advantages of slash-and-burn agriculture. This increase occurs noticeably earlier than the industrial revolution indicating that early humans may have impacted the Earth System even earlier than the currently accepted timeline. This evidence suggests that a more robust definition of the Anthropocene can account for this.

## Bibliography


Agenbroad, L. D. (2018, December 7). *Holocene epoch | Causes, Effects, & Facts*. Encyclopedia Britannica. https://www.britannica.com/science/Holocene-Epoch

Aleman, J. C., Blarquez, O., Bentaleb, I., Bonté, P., Brossier, B., Carcaillet, C., Gond, V., Gourlet-Fleury, S., Kpolita, A., Lefèvre, I., Oslisly, R., Power, M. J., Yongo, O., Bremond, L., & Favier, C. (2013). Tracking land-cover changes with sedimentary charcoal in the Afrotropics. *The Holocene*, *23*(12), 1853–1862. https://doi.org/10.1177/0959683613508159

Arienzo, M. M., McConnell, J. R., Murphy, L. N., Chellman, N., Das, S., Kipfstuhl, S., & Mulvaney, R. (2017). Holocene black carbon in Antarctica paralleled Southern Hemisphere climate. *Journal of Geophysical Research: Atmospheres*, *122*(13), 6713–6728. https://doi.org/10.1002/2017jd026599

Battistel, D., Kehrwald, N. M., Zennaro, P., Pellegrino, G., Barbaro, E., Zangrando, R., Pedeli, X. X., Varin, C., Spolaor, A., Vallelonga, P. T., Gambaro, A., & Barbante, C. (2018). High-latitude Southern Hemisphere fire history during the mid- to late Holocene (6000–750 BP). *Climate of the Past*, *14*(6), 871–886. https://doi.org/10.5194/cp-14-871-2018

Bender, M., Sowers, T., & Brook, E. (1997). Gases in ice cores. *Proceedings of the National Academy of Sciences*, *94*(16), 8343–8349. https://doi.org/10.1073/pnas.94.16.8343

Blaauw, M., & Christen, J. A. (2011). Flexible paleoclimate age-depth models using an autoregressive gamma process. *Bayesian Analysis*, *6*(3), 457–474. https://doi.org/10.1214/11-ba618

Blarquez, O., Vannière, B., Marlon, J. R., Daniau, A. L., Power, M. J., Brewer, S., & Bartlein, P. J. (2014). paleofire: An R package to analyse sedimentary charcoal records from the Global Charcoal Database to reconstruct past biomass burning. *Computers & Geosciences*, *72*, 255–261. https://doi.org/10.1016/j.cageo.2014.07.020

Bock, M., Schmitt, J., Beck, J., Seth, B., Chappellaz, J., & Fischer, H. (2017). Glacial/interglacial wetland, biomass burning, and geologic methane emissions constrained by dual stable isotopic CH4ice core records. *Proceedings of the National Academy of Sciences*, *114*(29), E5778–E5786. https://doi.org/10.1073/pnas.1613883114

Bond, T. C., Doherty, S. J., Fahey, D. W., Forster, P. M., Berntsen, T., DeAngelo, B. J., Flanner, M. G., Ghan, S., Kärcher, B., Koch, D., Kinne, S., Kondo, Y., Quinn, P. K., Sarofim, M. C., Schultz, M. G., Schulz, M., Venkataraman, C., Zhang, H., Zhang, S., . . . Zender, C. S. (2013). Bounding the role of black carbon in the climate system: A scientific assessment. *Journal of Geophysical Research: Atmospheres*, *118*(11), 5380–5552. https://doi.org/10.1002/jgrd.50171

Brovkin, V., Lorenz, S., Raddatz, T., Ilyina, T., Stemmler, I., Toohey, M., & Claussen, M. (2019). What was the source of the atmospheric CO2 increase during the Holocene? *Biogeosciences*, *16*(13), 2543–2555. https://doi.org/10.5194/bg-16-2543-2019

Buis, B. N. A. J. P. L. (2021, February 24). *Milankovitch (Orbital) Cycles and Their Role in Earth's Climate*. Climate Change: Vital Signs of the Planet. https://climate.nasa.gov/news/2948/milankovitch-orbital-cycles-and-their-role-in-earths-climate/#:%7E:text=Eccentricity%20measures%20how%20much%20the,between%20Earth%20and%20the%20Sun.&text=The%20total%20change%20in%20global,eccentricity%20cycle%20is%20very%20small.

Cael, B. B., & Seekell, D. A. (2016). The size-distribution of Earth's lakes. *Scientific Reports*, *6*(1), 1–3. https://doi.org/10.1038/srep29633

Campisano, C. J. (2012). *Milankovitch Cycles, Paleoclimatic Change, and Hominin Evolution | Learn Science at Scitable*. The Nature Education: Knowledge Project. https://www.nature.com/scitable/knowledge/library/milankovitch-cycles-paleoclimatic-change-and-hominin-evolution-68244581/?error=cookies_not_supported&code=eaff7355-2f38-45b0-b327-86af20e1a1f5

Chappellaz, J. A., Fung, I. Y., & Thompson, A. M. (1993). The atmospheric CH4 increase since the Last Glacial Maximum. *Tellus B: Chemical and Physical Meteorology*, *45*(3), 228–241. https://doi.org/10.3402/tellusb.v45i3.15726

Chaubey, J. P., Moorthy, K. K., Babu, S. S., Nair, V. S., & Tiwari, A. (2010). Black carbon aerosols over coastal Antarctica and its scavenging by snow during the Southern Hemispheric summer. *Journal of Geophysical Research*, *115*(D10), 1–16. https://doi.org/10.1029/2009jd013381

Daniau, A. L., Bartlein, P. J., Harrison, S. P., Prentice, I. C., Brewer, S., Friedlingstein, P., Harrison-Prentice, T. I., Inoue, J., Izumi, K., Marlon, J. R., Mooney, S., Power, M. J., Stevenson, J., Tinner, W., Andrič, M., Atanassova, J., Behling, H., Black, M., Blarquez, O., . . . Zhang, Y. (2012). Predictability of biomass burning in response to climate changes. *Global Biogeochemical Cycles*, *26*(4), 1–12. https://doi.org/10.1029/2011gb004249

Dargaud, G., & Dargaud, J. (2004). *Dome C FAQ*. Guillaume & Jennifer Dargaud's Website. http://www.gdargaud.net/Antarctica/DomeCFAQ.html#Where

Gambaro, A., Zangrando, R., Gabrielli, P., Barbante, C., & Cescon, P. (2008). Direct Determination of Levoglucosan at the Picogram per Milliliter Level in Antarctic Ice by High-Performance Liquid Chromatography/Electrospray Ionization Triple Quadrupole Mass Spectrometry. *Analytical Chemistry*, *80*(5), 1649–1655. https://doi.org/10.1021/ac701655x

Gomez, B., Carter, L., Orpin, A. R., Cobb, K. M., Page, M. J., Trustrum, N. A., & Palmer, A. S. (2011). ENSO/SAM interactions during the middle and late Holocene. *The Holocene*, *22*(1), 23–30. https://doi.org/10.1177/0959683611405241

Gong, D., & Wang, S. (1999). Definition of Antarctic Oscillation index. *Geophysical Research Letters*, *26*(4), 459–462. https://doi.org/10.1029/1999gl900003

Hammes, K., Schmidt, M. W. I., Smernik, R. J., Currie, L. A., Ball, W. P., Nguyen, T. H., Louchouarn, P., Houel, S., Gustafsson, R., Elmquist, M., Cornelissen, G., Skjemstad, J. O., Masiello, C. A., Song, J., Peng, P., Mitra, S., Dunn, J. C., Hatcher, P. G., Hockaday, W. C., . . . Ding, L. (2007). Comparison of quantification methods to measure fire-derived (black/elemental) carbon in soils and sediments using reference materials from soil, water, sediment and the atmosphere. *Global Biogeochemical Cycles*, *21*(3), 1–18. https://doi.org/10.1029/2006gb002914

Harrison, S. P., & Prentice, C. I. (2003). Climate and CO2 controls on global vegetation distribution at the last glacial maximum: analysis based on palaeovegetation data, biome modelling and palaeoclimate simulations. *Global Change Biology*, *9*(7), 983–1004. https://doi.org/10.1046/j.1365-2486.2003.00640.x

Hennigan, C. J., Sullivan, A. P., Collett, J. L., & Robinson, A. L. (2010). Levoglucosan stability in biomass burning particles exposed to hydroxyl radicals. *Geophysical Research Letters*, *37*(9), 1–4. https://doi.org/10.1029/2010gl043088

Hoffmann, D., Tilgner, A., Iinuma, Y., & Herrmann, H. (2010). Atmospheric Stability of Levoglucosan: A Detailed Laboratory and Modeling Study. *Environmental Science & Technology*, *44*(2), 694–699. https://doi.org/10.1021/es902476f

Hu, Q. H., Xie, Z. Q., Wang, X. M., Kang, H., & Zhang, P. (2013). Levoglucosan indicates high levels of biomass burning aerosols over oceans from the Arctic to Antarctic. *Scientific Reports*, *3*(1), 1–7. https://doi.org/10.1038/srep03119

Iglesias, V., & Whitlock, C. (2014). Fire responses to postglacial climate change and human impact in northern Patagonia (41–43°S). *Proceedings of the National Academy of Sciences*, *111*(51), E5545–E5554. https://doi.org/10.1073/pnas.1410443111

Itabaiana Jr., I., Avelar do Nascimento, M., de Souza, R. O. M. A., Dufour, A., & Wojcieszak, R. (2020). Levoglucosan: a promising platform molecule? *Green Chemistry*, *22*(18), 5859–5880. https://doi.org/10.1039/d0gc01490g

Koch, D., Bond, T. C., Streets, D., Unger, N., & van der Werf, G. R. (2007). Global impacts of aerosols from particular source regions and sectors. *Journal of Geophysical Research*, *112*(D2), 1–24. https://doi.org/10.1029/2005jd007024

Kuo, L. J., Herbert, B. E., & Louchouarn, P. (2008). Can levoglucosan be used to characterize and quantify char/charcoal black carbon in environmental media? *Organic Geochemistry*, *39*(10), 1466–1478. https://doi.org/10.1016/j.orggeochem.2008.04.026

Leys, B. A., Marlon, J. R., Umbanhowar, C., & Vannière, B. (2018). Global fire history of grassland biomes. *Ecology and Evolution*, *8*(17), 8831–8852. https://doi.org/10.1002/ece3.4394

Long, C. M., Nascarella, M. A., & Valberg, P. A. (2013). Carbon black vs. black carbon and other airborne materials containing elemental carbon: Physical and chemical distinctions. *Environmental Pollution*, *181*, 271–286. https://doi.org/10.1016/j.envpol.2013.06.009

Loulergue, L., Parrenin, F., Blunier, T., Barnola, J. M., Spahni, R., Schilt, A., Raisbeck, G., & Chappellaz, J. (2007). New constraints on the gas age-ice age difference along the EPICA ice cores, 0–50 kyr. *Climate of the Past*, *3*(3), 527–540. https://doi.org/10.5194/cp-3-527-2007

Mariani, M., & Fletcher, M. S. (2017). Long-term climate dynamics in the extra-tropics of the South Pacific revealed from sedimentary charcoal analysis. *Quaternary Science Reviews*, *173*, 181–192. https://doi.org/10.1016/j.quascirev.2017.08.007

Markle, B. R., Bertler, N. A. N., Sinclair, K. E., & Sneed, S. B. (2012). Synoptic variability in the Ross Sea region, Antarctica, as seen from back-trajectory modeling and ice core analysis. *Journal of Geophysical Research: Atmospheres*, *117*(D2), 1–17. https://doi.org/10.1029/2011jd016437

Marlon, J. R. (2020). What the past can say about the present and future of fire. *Quaternary Research*, *96*, 66–87. https://doi.org/10.1017/qua.2020.48

Marlon, J. R., Bartlein, P. J., Daniau, A. L., Harrison, S. P., Maezumi, S. Y., Power, M. J., Tinner, W., & Vanniére, B. (2013a). Global biomass burning: a synthesis and review of Holocene paleofire records and their controls. *Quaternary Science Reviews*, *65*, 5–25. https://doi.org/10.1016/j.quascirev.2012.11.029

Marlon, J. R., Bartlein, P. J., Daniau, A. L., Harrison, S. P., Maezumi, S. Y., Power, M. J., Tinner, W., & Vanniére, B. (2013b). Global biomass burning: a synthesis and review of Holocene paleofire records and their controls. *Quaternary Science Reviews*, *65*, 5–25. https://doi.org/10.1016/j.quascirev.2012.11.029

Marshall, G. J. (2007). Half-century seasonal relationships between the Southern Annular mode and Antarctic temperatures. *International Journal of Climatology*, *27*(3), 373–383. https://doi.org/10.1002/joc.1407

Marshall, G. J., & Thompson, D. W. J. (2016). The signatures of large-scale patterns of atmospheric variability in Antarctic surface temperatures. *Journal of Geophysical Research: Atmospheres*, *121*(7), 3276–3289. https://doi.org/10.1002/2015jd024665

Masson-Delmotte, V., Buiron, D., Ekaykin, A., Frezzotti, M., Gallée, H., Jouzel, J., Krinner, G., Landais, A., Motoyama, H., Oerter, H., Pol, K., Pollard, D., Ritz, C., Schlosser, E., Sime, L. C., Sodemann, H., Stenni, B., Uemura, R., & Vimeux, F. (2011). A comparison of the present and last interglacial periods in six Antarctic ice cores. *Climate of the Past*, *7*(2), 397–423. https://doi.org/10.5194/cp-7-397-2011

May, A., Eschenbach, W., Eschenbach, W., Watts, A., Worrall, E., Rotter, C., Rotter, C., Rotter, C., & Worrall, E. (2017, June 6). *A Holocene Temperature Reconstruction Part 2: More reconstructions*. Watts Up With That? https://wattsupwiththat.com/2017/06/06/a-holocene-temperature-reconstruction-part-2-more-reconstructions/

Muñoz-Díaz, D., & Rodrigo, F. (2005). Influence of the El Niño-Southern Oscillation on the probability of dry and wet seasons in Spain. *Climate Research*, *30*, 1–12. https://doi.org/10.3354/cr030001

Oris, F., Ali, A. A., Asselin, H., Paradis, L., Bergeron, Y., & Finsinger, W. (2014). Charcoal dispersion and deposition in boreal lakes from 3 years of monitoring: Differences between local and regional fires. *Geophysical Research Letters*, *41*(19), 6743–6752. https://doi.org/10.1002/2014gl060984

Parish, T. R., & Bromwich, D. H. (2007). Reexamination of the Near-Surface Airflow over the Antarctic Continent and Implications on Atmospheric Circulations at High Southern Latitudes*. *Monthly Weather Review*, *135*(5), 1961–1973. https://doi.org/10.1175/mwr3374.1

Parish, T. R., & Cassano, J. J. (2003). The Role of Katabatic Winds on the Antarctic Surface Wind Regime. *Monthly Weather Review*, *131*(2), 317–333. https://doi.org/10.1175/1520-0493(2003)131<0317:TROKWO>2.0.CO;2

Parrenin, F., Barnola, J. M., Beer, J., Blunier, T., Castellano, E., Chappellaz, J., Dreyfus, G., Fischer, H., Fujita, S., Jouzel, J., Kawamura, K., Lemieux-Dudon, B., Loulergue, L., Masson-Delmotte, V., Narcisi, B., Petit, J. R., Raisbeck, G., Raynaud, D., Ruth, U., . . . Wolff, E. (2007). The EDC3 chronology for the EPICA Dome C ice core. *Climate of the Past*, *3*(3), 485–497. https://doi.org/10.5194/cp-3-485-2007

Power, M., Marlon, J., Bartlein, P., & Harrison, S. (2010). Fire history and the Global Charcoal Database: A new tool for hypothesis testing and data exploration. *Palaeogeography, Palaeoclimatology, Palaeoecology*, *291*(1–2), 52–59. https://doi.org/10.1016/j.palaeo.2009.09.014

Raisbeck, G. M., Yiou, F., Jouzel, J., & Stocker, T. F. (2007). Direct north-south synchronization of abrupt climate change record in ice cores using Beryllium 10. *Climate of the Past*, *3*(3), 541–547. https://doi.org/10.5194/cp-3-541-2007

Richerson, P. J., Boyd, R., & Bettinger, R. L. (2001). Was Agriculture Impossible during the Pleistocene but Mandatory during the Holocene? A Climate Change Hypothesis. *American Antiquity*, *66*(3), 387–411. https://doi.org/10.2307/2694241

Rintoul, S. R., Hughes, C. W., & Olbers, D. (2001). Chapter 4.6 The antarctic circumpolar current system. *International Geophysics*, 271–XXXVI. https://doi.org/10.1016/s0074-6142(01)80124-8

Roberts, N. (1999). Holocene epoch. *Encyclopedia of Earth Science*, 324. https://doi.org/10.1007/1-4020-4494-1_174

Sajwan, K. S., Punshon, T., & Seaman, J. C. (2006). Production of Coal Combustion Products and Their Potential Uses. *Coal Combustion Byproducts and Environmental Issues*, 3–9. https://doi.org/10.1007/0-387-32177-2_1

Scafetta, N. (2016). Problems in Modeling and Forecasting Climate Change: CMIP5 General Circulation Models versus a Semi-Empirical Model Based on Natural Oscillations. *International Journal of Heat and Technology*, *34*(S2), S435–S442. https://doi.org/10.18280/ijht.34s235

Schoenemann, S. W., Steig, E. J., Ding, Q., Markle, B. R., & Schauer, A. J. (2014). Triple water-isotopologue record from WAIS Divide, Antarctica: Controls on glacial-interglacial changes in17Oexcessof precipitation. *Journal of Geophysical Research: Atmospheres*, *119*(14), 8741–8763. https://doi.org/10.1002/2014jd021770

Shrestha, G., Traina, S., & Swanston, C. (2010). Black Carbon's Properties and Role in the Environment: A Comprehensive Review. *Sustainability*, *2*(1), 294–320. https://doi.org/10.3390/su2010294

Stenni, B., Masson-Delmotte, V., Selmo, E., Oerter, H., Meyer, H., Röthlisberger, R., Jouzel, J., Cattani, O., Falourd, S., Fischer, H., Hoffmann, G., Iacumin, P., Johnsen, S., Minster, B., & Udisti, R. (2010). The deuterium excess records of EPICA Dome C and Dronning Maud Land ice cores (East Antarctica). *Quaternary Science Reviews*, *29*(1–2), 146–159. https://doi.org/10.1016/j.quascirev.2009.10.009

Stephens, L., Fuller, D., Boivin, N., Rick, T., Gauthier, N., Kay, A., Marwick, B., Armstrong, C. G., Barton, C. M., Denham, T., Douglass, K., Driver, J., Janz, L., Roberts, P., Rogers, J. D., Thakar, H., Altaweel, M., Johnson, A. L., Sampietro Vattuone, M. M., . . . Ellis, E. (2019). Archaeological assessment reveals Earth's early transformation through land use. *Science*, *365*(6456), 897–902. https://doi.org/10.1126/science.aax1192

Stohl, A., & Sodemann, H. (2010). Characteristics of atmospheric transport into the Antarctic troposphere. *Journal of Geophysical Research*, *115*(D2), 1–16. https://doi.org/10.1029/2009jd012536

Sverdrup, H. U. (1947). Wind-Driven Currents in a Baroclinic Ocean; with Application to the Equatorial Currents of the Eastern Pacific. *Proceedings of the National Academy of Sciences*, *33*(11), 318–326. https://doi.org/10.1073/pnas.33.11.318

Timmermann, A., Friedrich, T., Timm, O. E., Chikamoto, M. O., Abe-Ouchi, A., & Ganopolski, A. (2014). Modeling Obliquity and CO2 Effects on Southern Hemisphere Climate during the Past 408 ka*. *Journal of Climate*, *27*(5), 1863–1875. https://doi.org/10.1175/jcli-d-13-00311.1

Yao, P., Schwab, V. F., Roth, V. N., Xu, B., Yao, T., & Gleixner, G. (2013). Levoglucosan concentrations in ice-core samples from the Tibetan Plateau determined by reverse-phase high-performance liquid chromatography–mass spectrometry. *Journal of Glaciology*, *59*(216), 599–612. https://doi.org/10.3189/2013jog12j157

Zennaro, P., Kehrwald, N., Marlon, J., Ruddiman, W. F., Brücher, T., Agostinelli, C., Dahl-Jensen, D., Zangrando, R., Gambaro, A., & Barbante, C. (2015). Europe on fire three thousand years ago: Arson or climate? *Geophysical Research Letters*, *42*(12), 5023–2033. https://doi.org/10.1002/2015gl064259

Zennaro, P., Kehrwald, N., McConnell, J. R., Schüpbach, S., Maselli, O. J., Marlon, J., Vallelonga, P., Leuenberger, D., Zangrando, R., Spolaor, A., Borrotti, M., Barbaro, E., Gambaro, A., & Barbante, C. (2014). Fire in ice: two millennia of boreal forest fire history from the Greenland NEEM ice core. *Climate of the Past*, *10*(5), 1905–1924. https://doi.org/10.5194/cp-10-1905-2014